JPP JOURNAL OF PROTEINS AND PROTEOMICS
2(2), July-December 2011, pp. 145-169

FLUORESCENCE CORRELATION SPECTROSCOPY: A BRIEF REVIEW OF TECHNIQUES AND APPLICATIONS TO BIOMOLECULES AND BIOSYSTEMS

Pramit K Chowdhury

Department of Chemistry, Indian Institute of Technology Delhi, Hauz Khas, New Delhi 110016, India

Abstract: Fluorescence correlation spectroscopy is a non-invasive technique and is based on fluctuations of fluorescence within a tiny observation volume under equilibrium conditions. With its wide applicability both *in vitro* and *in vivo*, it is gradually becoming one of the most sought after spectroscopic methods among the scientific community. Processes due to diffusion (translation and rotation), chemical reactions, excited state photophysical process like triplet blinking and isomerization, binding studies and conformational dynamics of biomolecules can all be monitored using FCS thus confirming the versatility of the technique. Additionally with the advancement in instrumentation and electronics, FCS studies can be carried out with a high degree of spatial and temporal resolution thereby further improving the efficacy of the technique. Here an overview of the basics of FCS, along with variations in instrumentation has been presented. The varied applications of the technique mostly with regards to biomolecules and biosystems have also been reviewed.

Keywords: Fluctuations; Autocorrelation; Cross-correlation; Confocal ; Protein aggregation; Protein dynamics; Diffusion; Membranes.

1. Introduction

Since the formulation and conceptualization by Magde and Elson (Magde *et al.* 1972; Elson *et al.* 1974; Magde *et al.* 1974) fluorescence correlation spectroscopy has come a long way and now is probably one of the widest and most frequently used techniques for probing a variety of phenomena. FCS is based on the fluctuation of the number of photons arriving at the detector and their subsequent correlation, with fluctuations arising from a host of processes like, diffusion (translational and rotational), chemical reactions, excited state photophysics and many more (Magde, 1976; Webb, 1976; Thompson, 1991; Krichevsky *et al.*, 2002; Elson, 2001; Hess *et al.*, 2002; Schwille, 2002; Kim *et al.*, 2003; Bacia *et al.*, 2003; Haustein *et al.*, 2003; Haustein *et al.*, 2007; Mütze *et al.*, 2011). One of the biggest advantages of this technique is that not only is it non-invasive but also the equilibrium fluctuations are spontaneous in nature and governed solely by external conditions and environment. In other words any such process that might give rise to an observable fluctuation in fluorescence can be potentially monitored by FCS and hence makes this technique suitable for a vast range of processes. As an analytical tool FCS underwent a dramatic facelift with the development of the confocal microscope by Rigler and coworkers in their pioneering efforts towards single molecule detection (Rigler *et al.*, 1990a; Rigler *et al.*, 1990b).

The theory behind FCS has been developed in extensive detail in a number of excellent reviews (Elson *at al.*, 1974; Webb, 1976; Thompson, 1991; Krichevsky *et al.*, 2002), hence no attempt will be made here in that regard. Instead I will provide a short synopsis of the essentials of the theory and point out some of the significant features and variations that have been used extensively for FCS analyses over the years. In FCS one compares (or correlates) the temporal self-similarity of the fluctuations around equilibrium and is characterized by the second-

Corresponding Author: **Pramit K Chowdhury**
E-mail: pramitc@chemistry.iitd.ac.in

order normalized autocorrelation function, $G(\tau)$ which is expressed as:

$$G(\tau) = \frac{\langle \delta F(t) \delta F(t+\tau) \rangle}{\langle F(t) \rangle^2} \quad (1)$$

where $\delta F(t) = F(t) - \langle F(t) \rangle$ is the fluctuation in fluorescence from the temporal average $\langle F(t) \rangle = \frac{1}{T}\int_0^T F(t)dt$ of the signal as defined. τ is referred to as the lag time as a function of which the self-similarity in signal is measured **(Fig. 1)**. Thus as evident from the expression, the correlation will be the maximum at the shortest lag times while the same will undergo decay with increase in *t*. If the fluctuation is only due to concentration effects, that is, diffusion of species into and out of a well-defined confocal volume (~ 1fL), then assuming a three dimensional (3D) Gaussian excitation profile, the following expression for $G(\tau)$ for a system undergoing single component diffusion has been derived (Krichevsky, *et al.*, 2002; Kim *et al.*, 2003; Bacia *et al.*, 2003; Haustein *at al.*, 2003, 2007).

$$G_{diff}(\tau) = \frac{1}{N}\left(1 + \frac{\tau}{\tau_D}\right)^{-1}\left(1 + \frac{\tau}{\omega^2 \tau_D}\right)^{-1/2} \quad (2)$$

where N is the number of fluctuating molecules in the confocal (detection) volume averaged over the time of the experiment and ω is a characteristic of the system known as the aspect ratio of the volume and is given by $\omega = \frac{\omega_z}{\omega_{xy}}$. ω_z and ω_{xy} are the $1/e^2$ beam waists in the axial and radial directions of the illumination volume respectively. The effective illuminated/detection volume can be expressed as $V = \pi^{3/2}\omega_{xy}^2\omega_z$. τ_D is the characteristic diffusion time in the lateral direction and is related to the diffusion coefficient D of the species under investigation by the relation

$\tau_D = \frac{\omega_{xy}^2}{4D}$ [for two–photon excitation (Haustein *et al.*, 2007) $\tau_D = \frac{\omega_{xy}^2}{8D}$] (3)

For a spherical particle, from Stokes-Einstein's equation one can calculate the hydrodynamic radius R_h as follows:

$$D = \frac{kT}{6\pi\eta R_h} \quad (4)$$

where k is the Boltzmann's constant, T is the temperature and η is the viscosity of the medium wherein diffusion occurs. Thus using FCS one can easily get an idea of the sizes of the respective diffusing particles and/or the viscosity of the medium, from the diffusion times so obtained on analysis of the autocorrelation curves. Moreover it is worth noting that for $\tau = 0, G(0) = \frac{1}{N}$ (from eqn. 2), thus signifying that if the dimensions of the confocal volume are known, the concentration of the molecules can also be determined.

For single component 2D diffusion as is often the case for diffusion in membranes, the expression for $G(\tau)$ becomes

$$G_{diff}(\tau) = \frac{1}{N}\left(1 + \frac{\tau}{\tau_D}\right)^{-1} \quad (5)$$

The above expressions for $G(\tau)$ were derived based on the assumption that diffusion is the only source of fluctuation. However additional fluctuations due to photophysical processes like intersystem crossing to the triplet state (**Fig. 2**) and fluctuations arising from rotational diffusion which are much faster than translational diffusion are also observed frequently. Hence to account for these, the modified autocorrelation function can be written as (Mütze *et al.*, 2011)

$$G(\tau) = G_{fast}(\tau) G_{diff}(\tau) \quad (6)$$

Most of the fluorophores used for FCS measurements show triplet state dynamics to different extents. During the transition to triplet state, the fluorophore is in a dark state and becomes visible only when re-excited after decaying to the ground singlet state. This switching between on and off mode results in what is popularly termed as triplet blinking and

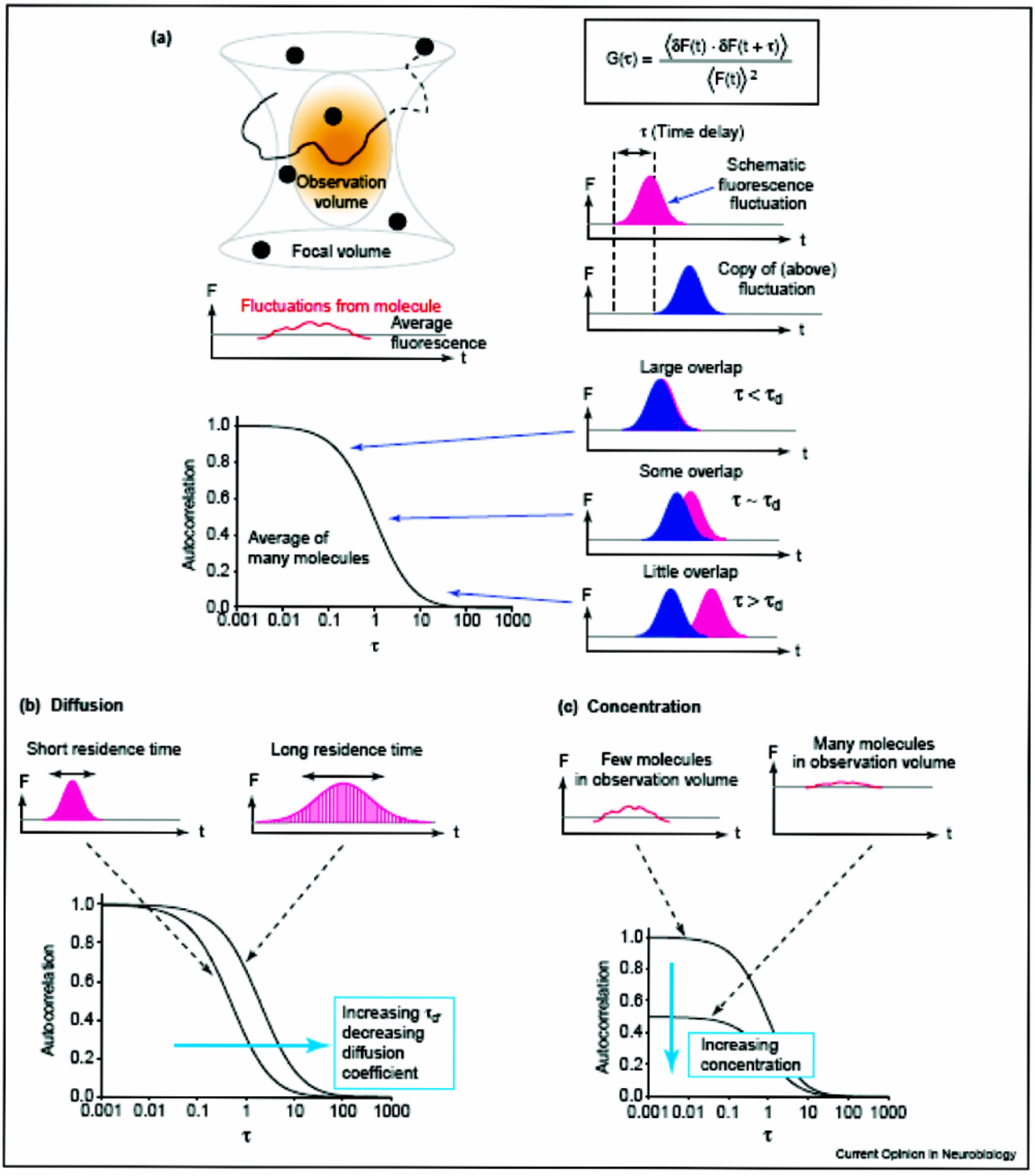

Figure 1: General Principles of FCS (Adapted from Kim *et al.*, 2003). (a) Representation of a confocal volume showing particles diffusing in and out giving rise to fluctuations in fluorescence. Fluctuations (**δF(t)) from average fluorescence (<F(t)>) are represented in the schematic below the confocal volume. Development of the autocorrelation decay as a function of time delay is shown to the right of the confocal volume. As mentioned in the text shorter time delays lead to maximum overlap and hence high correlation while longer time delays result in lower correlation arising from reduced extent of overlap. (b) Effect of residence time on the autocorrelation curve. The larger the residence time, the slower is the decay of the autocorrelation function and hence larger is the recovered diffusion time. The half-value decay time gives an estimate of the mean diffusion time, τ_D. (c) Effect of concentration. Lower concentration leads to higher correlation amplitude because of larger fluctuations; on the contrary very high concentrations leads to high average fluorescence and hence reduction in fluctuations along with decrease in the correlation amplitude**

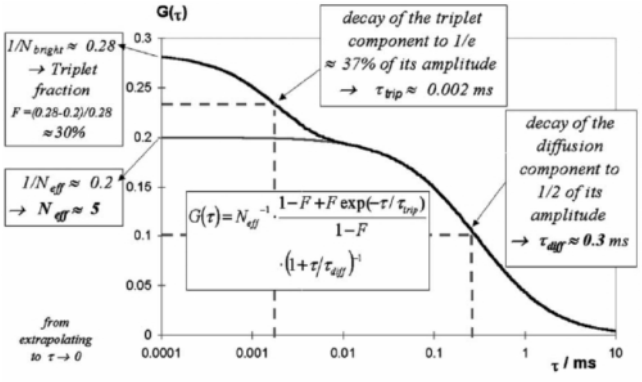

Figure 2: **Parameters in a simple autocorrelation curve. Computed fluorescence correlation curve for two-dimensional diffusion including triplet blinking. Evidently, the reciprocal of the number of particles in the detection volume determines the amplitude of the FCS curve; the kinetics of the triplet blinking process (relaxation time τ_{trip}) and the particle mobility (diffusion time τ_{diff}) determine the two characteristic decays in this curve. (Adapted from Bacia *et al.*, 2003)**

gives rise to a component in the autocorrelation trace that is characteristic of the triplet state relaxation of the dye molecule. Many studies with regards to the dependence of the amplitude of this triplet component on conditions like excitation laser power and reaction conditions already exist (Widengren *et al.*, 1995; Davis *et al.*, 2006). To take into account the triplet fluctuation contribution, the fast correlation component can be written as

$$G_{fast}(\tau) = \frac{1 - F + F\exp\left(-\tau/\tau_F\right)}{1 - F} \qquad (7)$$

with τ_F and F representing the triplet time constant and triplet amplitude respectively.

Another aspect wherein FCS provides a distinct advantage is in measuring the rotational diffusion of molecules traversing the detection volume. For a system exhibiting both fluctuations due to rotational diffusion and triplet dynamics (or other comparable fast processes), the combined autocorrelation function resulting from the faster fluctuations can be expressed as (Widengren *et al.*, 1999)

$$G_{fast}(\tau) = \left[1 + \mathrm{Re}\,xp\left(\frac{-\tau}{\tau_R}\right)\right]\left[\frac{1 - F + F\exp\left(-\tau/\tau_F\right)}{1 - F}\right] \qquad (8)$$

with τ_R being the rotational correlation time and R being the amplitude of the process. Time resolved anisotropy measurements also provide direct information about the rotations of molecules but suffer from the intrinsic drawback of being limited by the lifetime of the fluorophore. However FCS suffers from no such disadvantage as it only depends on the fluctuation timescale and hence can more reliably provide information about the rotation of molecules (Krichevsky *et al.*, 2002). While only a few studies using FCS for rotational measurements exist (Ehrenberg *et al.*, 1974; Aragon *et al.*, 1975; Ehrenberg *et al.*, 1976; Kask *et al.*, 1987; Kask *et al.*, 1988; Barcellona *et al.*, 2004; Anastasia *et al.*, 2010), a recent report on its application to measure the rotation of peptide-coated nanorods further confirms the advantage of FCS in measuring rotational diffusion (Tsay *et al.* 2006). Shown in **Fig. 3** is a summary of the different timescales of processes that can be monitored using FCS, in which the anti-bunching phenomenon is characterized by a dip in the correlation curve. The anti-bunching process is the fastest time that can be measured using FCS and arises from the fact that once a photon is emitted, the fluorophore will have to undergo another excitation cycle before it can release a second photon (Krichevsky *et al.*, 2002; Gösch *et al.*, 2005). Moreover, it should be kept in mind that while diffusion is directly related to the confocal volume, however exponential relaxation processes (the so called fast processes) like rotational diffusion, triplet photodynamics are independent of the dimensions of the volume element.

Since diffusion measurements using FCS is based on the analyses of fluctuations of molecules into and out of the confocal volume, the concentration range over which experiments can be carried out is also critical. For concentrations that are too high, the confocal volume will always remain occupied with emitting fluorophores giving rise to a high background signal and thus making fluctuations $\delta F(t)$ almost insignificant (**Fig. 1**). On the other hand, if the concentration is too low, the number of photons available for correlation will also be quite limited thus decreasing the signal-to-noise ratio and thereby increasing the experimental data acquisition time. Thus for FCS the concentration should ideally be in the range of higher picomolar to lower nanomolar depending on the brightness of the

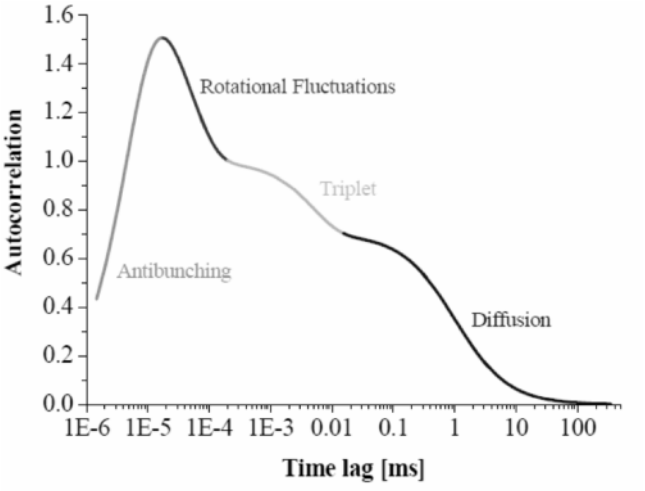

Figure 3: **Timescales of various processes that can be monitored by analysis of the autocorrelation curves of the FCS measurements (Adapted from Schwille *et al.*, 2004). The antibunching is featured by an anti-correlation (dip in the FCS trace) at very fast times thus further reinforcing the single molecule nature of the measurements**

fluorophore. Vogel and coworkers have shown that to distinguish two species having different diffusion coefficients using FCS, a number of factors have to be taken into consideration. For species having high brightness, the diffusion times have to differ at least by a factor of 1.6 to be able to be distinguished. However for a mixture wherein the fluorescence count rate is low, the diffusion times need to differ by a factor of 8. This signifies that depending on the brightness of the species under investigation, the molecular masses have to differ by a factor of 4 to 500 (based on the fact that the diffusion time $\tau_D \propto M^{1/3}$) to resolve the two species (Meseth *et al.*, 1999). Furthermore, Landes and coworkers show that to obtain reliable diffusion times through FCS for complex systems, the choice of lag time(s) and autocorrelation average time(s) can have a significant effect on the observed correlation curves. According to the authors the minimum lag time (τ_{min}) should not exceed two-thirds of the value of the characteristic diffusion time. On the other hand, the maximum lag time (τ_{max}) should at least be 5000 times greater than the expected diffusion time. Hence for a heterogeneous system composed of multiple diffusing entities, τ_{min} and τ_{max} must be maintained with respect to the fastest and slowest diffusing species respectively (Tcherniak *et al.* 2009). A series of theoretical studies regarding under what conditions FCS can be considered to be a true single molecule technique provide some thought provoking insights into the technique (Földes-Papp, 2006, 2007).

A variation of fluorescence fluctuation spectroscopy that is used very widely nowadays, in particular with respect to binding studies, is fluorescence cross correlation spectroscopy. While the concept is exactly similar to that of the conventional FCS technique, however for FCCS the correlation is carried out generally between photons of two different colours (the dual colour cross correlation technique) detected in two different channels (detectors). Thus the cross-correlation function is expressed as (Schwille *et al.*, 1997).

$$G_{cross}(\tau) = \frac{\langle \delta F_1(t) \delta F_2(t+\tau) \rangle}{\langle F_1(t) \rangle \langle F_2(t) \rangle} \qquad (9)$$

where the subscripts 1 and 2 refer to either two colours and/or two detectors (**Fig. 4**). This method was experimentally first realized by Rigler and coworkers wherein they observed the renaturation kinetics of two DNA complementary strands labeled with fluorophores of different colours (hence the name dual colour), namely rhoadmine green and Cyanine-5 (Cy5). A significant difference of the cross-correlation amplitude from that of autocorrelation is that for the former, the $G_{cross}(0)$ value increases with increase in concentration of bound species (**Fig. 4**) while the reverse happens for the latter (Schwille *et al.*, 1997; Schwille, 2001). The advantage of carrying out FCCS for binding studies can be further realized if the masses of the bound and unbound species and hence their respective diffusivities are not vastly different. Thus based on the aforesaid discussion on the resolution limits of FCS, if only one of the binding partners is labeled, then following its diffusion profile as a function of increase of bound species might not provide a clear picture as separation of bound and unbound species becomes difficult in the single colour FCS. Moreover, cross-correlation curves of two different colours have significantly reduced triplet amplitude as the probability of both dyes being in the triplet state simultaneously is quite small (Schwille *et al.* 1997). The applications of dual colour FCCS ranging from

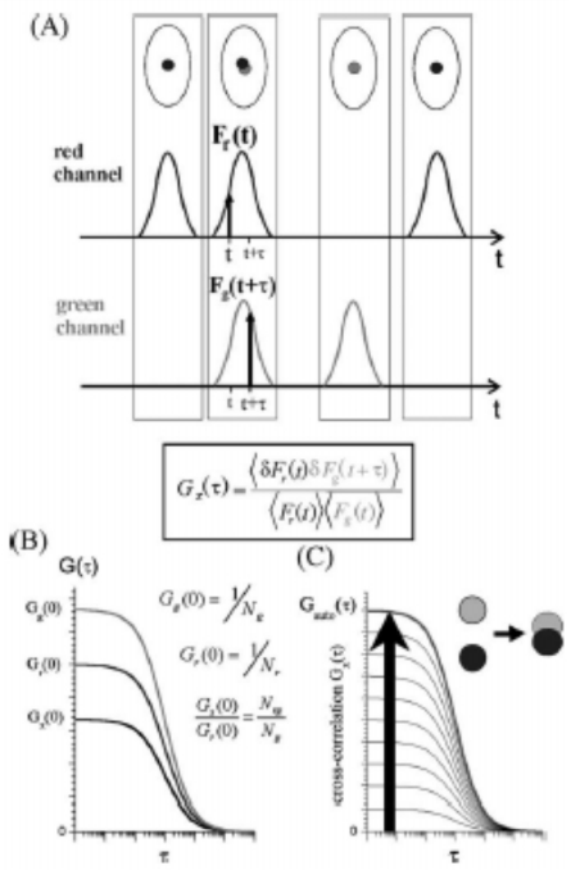

Figure 4: **Depiction of the cross-correlation concept involving two different fluorophores emitting in the green (g) and red (r) regions of the visible spectrum (Adapted from Bacia *et al.*, 2003). (A) Signals in the two detectors, that is, red and green channels arise from the individual red and green labeled species respectively along with the doubly labeled diffusing molecules. (B) $G_g(\tau)$ and $G_r(\tau)$ are the autocorrelation functions from the green and red-labeled entities respectively while $G_x(\tau)$ is the cross-correlation between the green and red labels. (C) The greater the fraction of bound species, the larger is the value of the cross-correlation amplitude relative to the individual autocorrelation amplitudes**

enzymatic cleavage to ligand binding and protein-protein association have been well reviewed by Schwille and coworkers. (Bacia *et al.*, 2006).

One of the major disadvantages of using the dual colour FCCS technique is the requirement of two excitation lasers being focused onto the sample simultaneously in a matter that they overlap. In this regard, Langowski and coworkers have provided a detailed analysis of the intrinsic advantages and drawbacks of the two-colour FCCS method (Wiedemann *et al.*, 2002). To circumvent this problem of spatial overlap of two lasers, single colour FCCS (two-photon) was developed wherein the tunable laser line of the Ti:Sapphire laser was used for exciting dyes of different colours (Schwille *et al.*, 2001;) Wohland and coworkers without using two-photon excitation but by careful selection of fluorophores showed that these can be excited simultaneously at a single laser wavelength, with as many as three different colours being detected, by using the 488 nm line of a continuous wave Argon-ion laser (Hwang *et al.*, 2006).

Two other methods based on fluorescence fluctuations namely, Photon counting histogram (PCH) and Fluorescence intensity distribution analysis (FIDA) have also been used extensively for fluctuation measurements. Both these methods are based on generating histograms of photon counts over defined sampling times (Chen *et al.*, 1999; Kask, *et al.*, 1999).

I would like to draw the attention of the readers here to the expression for the correlation function $G(\tau)$ for systems having multiple diffusing components. Under such conditions, the expression becomes (Krichevsky *et al.*, 2002).

$$G_{diff}(\tau) = \frac{1}{\left(\sum Q_k N_k\right)^2} \sum Q_j^2 N_j \left(1 + \frac{\tau}{\tau_{D_j}}\right)^{-1} \left(1 + \frac{\tau}{\omega^2 \tau_{D_j}}\right)^{-1/2} \quad (10)$$

where Q represents the quantum yield. It should therefore be noted that the amplitude of each species in the autocorrelation function is weighted by its respective quantum yield and hence data fitting and interpretation should be done with care in such cases.

2. Instrumentation Variations for FCS

The essential requirements for FCS instrumentation based on confocal microscopy involve a set of key components as shown (**Fig. 5**). The platform is composed of an inverted microscope to which laser(s) (both pulsed and continuous wave) can be coupled through one of the open ports (of the microscope). The laser wavelength depends upon the user's choice of fluorophores being excited in the respective measurements. The simplest setup (found in the earlier home-built FCS systems) uses a set of mirrors and lenses to guide the laser beam into

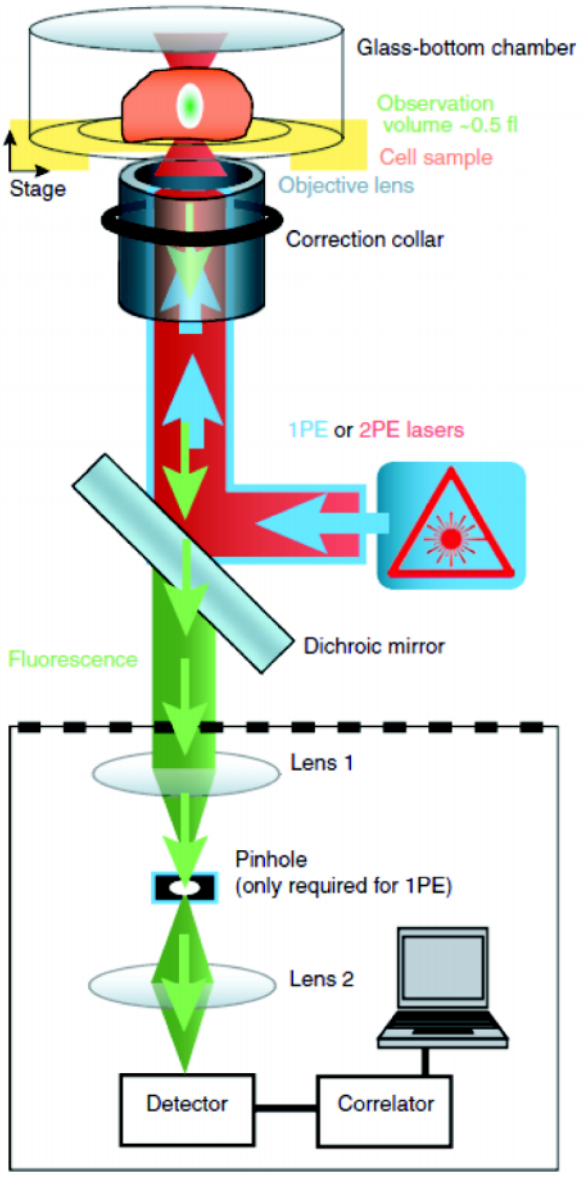

Figure 5: **A typical instrumental set-up for FCS measurements showing the basic components (Adapted from Kim *et al.*, 2007). 1PE and 2PE refer to one-photon and two-photon excitation lasers respectively (see text for details). The pinhole (referred to as the confocal pinhole) is a critical component for 1PE but is removed in case of 2PE. Instead of one-detector as shown here, two detectors can be easily integrated into the set-up for cross-correlation measurements. Alternatively a fiber coupler can replace the pinhole-second lens combination and be directly coupled to the detector. In this case the coupler aperture serves the role of the pinhole**

the back aperture of the microscope objective through a dichroic mirror. One of the important design issues that have to be kept in mind is the presence of a beam expander composed of two lenses that allows the user to overfill or underfill the back aperture of the objective (Helmchen *et al.*, 2005) Overfilling or underfilling can bring about differences in observation volumes with overfilling often giving rise to non-Gaussian beam profiles (see Hess *et al.*, 2002, for more details). The numerical aperture (NA) of the objective (either immersion oil or water based depending upon the application) is generally kept high (>1) to ensure maximum collection of the photons emitted by the fluorophores in the excitation volume. In the epifluorescence mode, the same dichroic mirror that guides the laser excitation beam into the objective is used to separate the fluorescence from unwanted excitation light. To ensure maximum attenuation of the laser excitation beam, another filter is used in the path of the emitted fluorescence after the dichroic to reject residual Rayleigh scattering. First-time users are encouraged to explore the website of Chroma Technology Corp (*www.chroma.com*) that provides excellent information on the types of filters/mirrors that need to be chosen for their specific application(s). Chroma also custom-makes mirrors on request for one's specific necessities, this being indeed a huge advantage for the varied fluorophores (often non-conventional) that can be obtained nowadays. Other companies that have also been extensively involved in such optical products are Newport Optics, Edmund Optics, Omega Optical and CVI Optics. The fluorescence emitted is focused onto a confocal pinhole that is placed in the image-plane to reject out-of-focus light. The pinhole provides resolution in the axial direction of the confocal volume and is an extremely important component for any confocal instrument. Subsequent to the confocal pinhole, the fluorescence is focused onto a detector with high quantum efficiency and capable of detecting single-photons. Avalanche photodiodes (the SPCM-AQR series) from Perkin-Elmer are the detectors of choice for this application and have a large wavelength range over which the quantum efficiency is quite high. Recent days are seeing a gradual shift of focus towards the development of array detectors for parallel single molecule measurements leading to high throughput assay (Gösch *et al.*, 2004). Other detectors showing single photon sensitivity for FCS include the PDM series from Microphoton Devices (www.microphotondevices.com), the 8-

channel SPAD module from Becker & Hickl and the hybrid GaAsP PMTs (Becker & Hickl). The hybrid PMTs allow FCS curves down to 100 ns correlation time (for a single detector) without the need of cross-correlation to avoid afterpulsing. In place of the confocal pinhole, the aperture of an optical fiber that feeds the emitted photons to the detector can also be used to act as the pinhole. The photons thus collected can be processed through hardware correlator cards like ALV-multiple tau correlator (www.alvgmbh.de, Langen, Germany) or those obtained from Correlator.com (www.correlator.com, New Jersey, USA) to get the resultant autocorrelation traces. Many groups have their own softwares wherein correlation is carried out after the photons are collected and binned with respect to their arrival times. Often with FCS systems having a single APD unit, spurious peaks resulting from detector afterpulsing are observed at timescales ≤ 1 μs thus preventing analyses of fast fluctuation dynamics (**Fig. 6**). In such cases, one can employ the cross-correlation set-up (another advantage of FCCS) wherein the emitted photons are split into two APDs using a non-polarising beamsplitter and the resultant photons from the detectors are correlated thus avoiding any effects of afterpulsing (Krichevsky *et al.*, 2002). Users are also advised to refer to the paper published in *Nature Protocol* by Schwille and coworkers wherein the authors provide a step-by-step guide towards performing FCS measurements (though this paper talks explicitly about FCS in cells, many of the aspects are also applicable for general FCS measurements) including a very thorough trouble-shooting section (Kim *et al.*, 2007). (Table 1 provides a list of companies having commercial FCS units).

2.1. NSOM FCS

Recent innovations have seen the development of techniques achieving resolution beyond the diffraction limited confocal microscopes. One such improvement is near-field optical scanning microscopy which has also been used recently for FCS measurements by the Lewis and Johnston groups (Lewis *et al.* 2003; Lewis *et al.* 2007; Vobornik *et al.*, 2008). Lewis *et al.* used a tapered cantilever optical fiber probe (aperture based) (**Fig. 7**) to obtain correlation traces from diffusing rhodamine dye molecules (Lewis *et al.* 2007) while the Johnston group showed that the NSOM-FCS observation area is at least an order of magnitude smaller than the confocal geometry. This method therefore offers a much better lateral and axial resolution and hence is extremely advantageous for studying spatial heterogeneity dependent diffusive processes in cells and membranes.

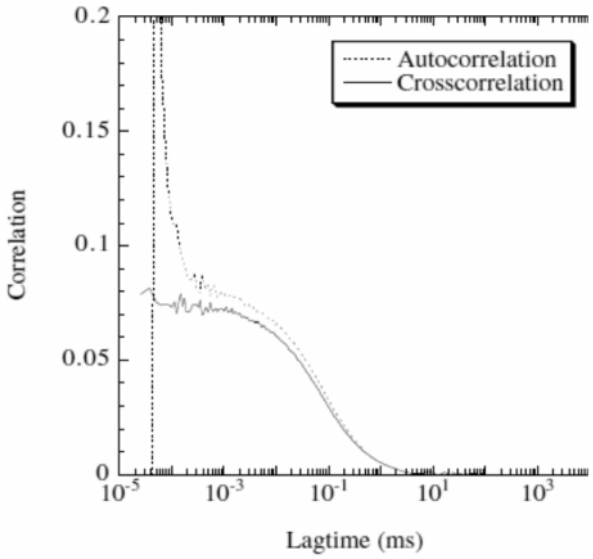

Figure 6: **Comparison of the auto- and cross-correlation curves using one and two APDs respectively for freely diffusing dye molecules (Adapted from Krichovksy *et al.*, 2002). The peak at ~100 ns arises due to afterpulsing of the detector and is completely eliminated in the cross-correlation mode thus signifying the usefulness for cross-correlation even in the standard FCS measurements**

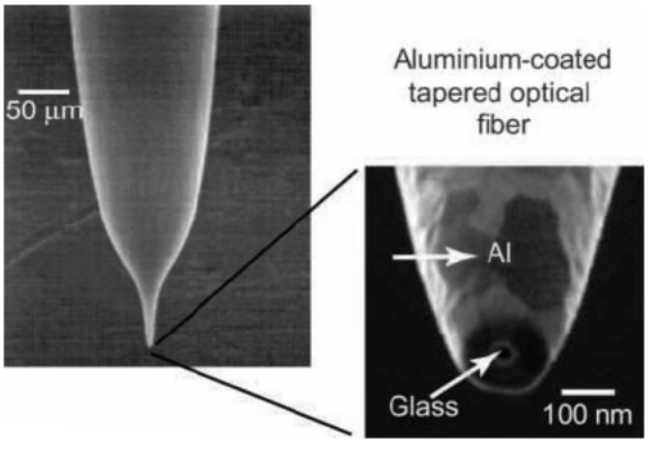

Figure 7: **Near-field optical probe (Adapted from de Lange *et al.*, 2001). It is generally prepared by pulling an optical fiber to a very thin diameter and then coating it with aluminum subsequent to which etching is carried out to get a circular end-region and an aperture. The aperture serves as the miniature light source and determines the optical resolution of the microscope**

Table 1
List of Companies and their Commercial Laser Scanning Microscopes along with FCS units

Company	*Website*	*Product Names*	*Remarks*
Olympus	www.olympusfluoview.com	Fluoview FV1000	Laser scanning microscope that can be fitted with FCS/FLIM attachments
Nikon	www.nikoninstruments.com/ Products/Microscope-Systems/ Confocal-Microscopes	C2 Confocal A1R-AR Confocal A1R MP Multiphoton Confocal	Point scanning microscope Line scanning microscope Equipped for mulitphoton excitation and imaging
Leica	www.leica-microsystems.com/ products/confocal-microscopes	TCS SP5 II TCS SMD FLCS	Broadband laser scanning system Combined FCS and FLIM single molecule detection (SMD) unit FLIM
		TCS SMD FLIM	FCS (and FCCS)
		TCS SMD FCS	Multiphoton microscope
		TCS SP5 MP	STED
		TCS-STED	(The FLCS, FLIM, FCS, MP and STED systems have SP5 II as the platform)
Zeiss	www.zeiss.de/micro	LSM 710 LSM 710 Confocor 3 ELYRA	Laser scanning microscope FCS attachment to LSM 710 PALM (Photoactivated Localization Microscopy and/or SR-SIM (Superresolution Structured Illumination) system for superresolution microscopy
PicoQuant	www.picoquant.com	Microtime 200 (with SymPhoTime software)	FCS, FLIM and FRET
		Compact Lifetime and FCS Upgrade Kit for LSMs	For: FV1000, TCS SP5, AI, C2 and LSM 710 laser scanning systems
Becker & Hickl	www.becker-hickl.de	DSC 120	Confocal FLIM (system comes equipped with galvano based mirrors for laser scanning microscopy)
		FLIM Upgrade Kit	For: FV1000, LSM 710 and TCS SP5 laser scanning systems
ISS	www.iss.com	Alba	Confocal Scanning FCS Allows PCH and is capable of single particle tracking

However the brightness per molecule in NSOM-FCS is approximately 10 times lower than that of confocal FCS thus requiring better probe design for NSOM to allow higher excitation intensities of the sample (Vobornik *et al.*, 2008). Application of NSOM-FCS on intact living cell membranes has further shown the advantage of this technique for studying dynamic processes with nanometer resolution (Manzo *et al.*, 2011).

2.2. *Two-photon FCS*

Two-photon microscopy offers significant advantages over the conventional one-photon technique. The principle of two-photon excitation is based on the simultaneous absorption of two photons that excite the molecule, the latter absorbing at a wavelength corresponding to the sum of the energies of the photons combined (Rubert, 2004; Helmchen *at al.*, 2005). One of the biggest advantages of two-photon over one-photon is the reduction in the excitation volume (**Fig. 8**). This aspect can easily be understood based on the fact that the signal for two-photon microscopy varies as the square of the light intensity (density of photons); hence when focused using a high NA objective, the maximum

photon flux occurs at the center of the focal spot (Oheim *at al.*, 2006). A drastic decrease in multiphoton processes is therefore seen just outside the focal region thereby giving rise to a very small excitation volume and hence much improved optical sectioning without the requirement of a confocal pinhole. Moreover since excitation takes place only at the focal spot, the photodamage of the absorbing fluorophores in the regions surrounding the spot is reduced to a significant extent (as opposed to that in conventional confocal microscopy where the illumination volume is much larger giving rise to increase photobleaching). However, one of the major drawbacks of the two-photon (or any multi-photon) technique is the cost involved as generation of high photon fluence at the focal spot typically requires the use of expensive ultrashort (~fs) lasers. The most widely used is the Titanium-sapphire oscillator with a broad wavelength tunability range of ~690 – 1100 nm thereby allowing the excitation of a large number of fluorophores. In one of the earliest applications of two-photon FCS, Gratton and coworkers probed the intracellular diffusion properties of latex beads in the cytoplasm of mouse fibroblast cells (Berland *et al.*, 1995). Indeed the greater penetration of the near-IR laser excitation light (Ti:sapphire) into cells or tissues without significant scattering because of reduced absorption of the long wavelength photons by autofluorescent species makes two-photon FCS ideal for *in vivo* applications. A comparative FCS study of mammalian and plant cells using one and two-photon excitations carried out by Schwille *at al.* clearly pointed out the aforesaid advantages of mutliphoton FCS (Schwille *at al.*, 1999). Schwille and Heinze used two-photon excitation to simultaneously excite fluorophores having distinct emission profiles and study their cross correlation properties (Schwille *et al.*, 2001). Nicoloni *et al.* monitored the reversibility of topological changes of lipid vesicles as a function of pressure using the same technique (Nicoloni *et al.* 2006). A significant disadvantage encountered in two-photon FCS is the enhanced photobleaching at the central focal spot due to the high peak power of the ultrashort excitation pulses (Nagy *et al.*, 2005).

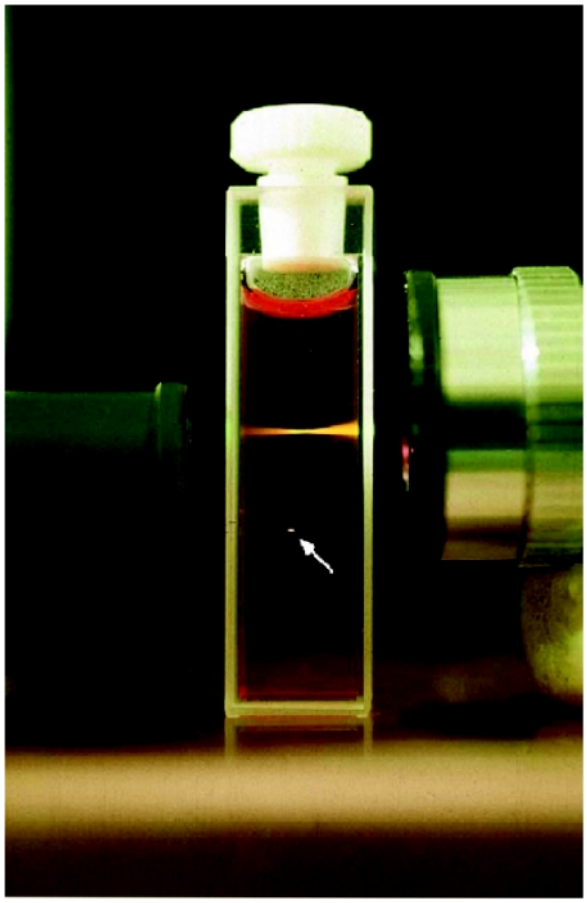

Figure 8: **A comparison between the sizes of the illumination volumes for one-photon and two-photon excitation (marked with arrow) (Adapted from Oheim *et al.*, 2006). Indeed two-photon excitation leads to a considerable decrease in detection volume (almost reduced to a spot as compared to the one-photon case) as evident**

2.3. STED-FCS

Another improvement over the spatial resolution obtained through confocal FCS is STED-FCS wherein Hell and coworkers have used the stimulated emission depletion (STED) technique to monitor fluorescence fluctuations of diffusing systems. STED uses a combination of synchronized pulses with the first one exciting the molecules to the higher energy state while the second pulse (sent in after a delay with respect to the first) depletes the excited state population by stimulating emission to the higher vibrational states of the ground level (Hell, 2007). This technique has been shown to bring about almost five-fold decrease in detection volume (as compared to a confocal microscope) with as much as 25-fold reduction in axial transit time, thus extending the applicability of far-field fluorescence fluctuation spectroscopy (FFS; this

is an alternate commonly used terminology for FCS) (Kastrup *et al.*, 2005). STED-FCS has also been used for monitoring diffusion of single lipid molecules of membranes in living cells (Eggeling *et al.*, 2009) and for studying nanoscale lipid interactions with a high degree of spatial resolution (Ringemann *et al.*, 2009). STED also allows modulation of the focal volume size by changing the power of the STED beam (Ringemann *et al.*, 2009) (the corresponding counter part in confocal microscopy is achieved by underfilling or overfilling the back-aperture which involves manual/automated tweaking of optics).

2.4. *TIR-FCS*

Total internal reflection microscopy (TIRFM) in combination with FCS (hence TIR-FCS) has widened the applicability range and usage of FCS to a significant extent. The excitation light for any TIR based microscopic method is the evanescent wave generated at the interface of two media having different indices of refraction (Thompson *et al.*, 2007). Since the evanescent wave depends exponentially on the distance of penetration into the medium with lower refractive index, thus its intensity decays quite rapidly as one moves away from the surface. In other words, TIRFM is best suited for probing surface phenomena. This is a distinct advantage over conventional one-photon microscopy wherein the axial spread of the illumination volume can be quite significant. TIR-FCS can be either prism based or objective based (**Fig. 9**). In the former, the excitation light is coupled to the surface of interest through a prism while in the latter the laser beam is focused through the periphery of an objective having high numerical aperture. Readers who want to know more about details of TIR-FCS setups are encouraged to look up the excellent reviews by Thompson and coworkers (Thompson *et al.*, 2007; Thompson *et al.*, 2009). Seeger and coworkers using a parabolic mirror objective have achieved volumes as low as 5 attoliters thus further improving spatial resolution by orders of magnitude as compared to a confocal microscope (Ruckstuhl *et al.*, 2004).

2.5. *FLCS*

Fluorescence lifetime correlation spectroscopy (FLCS) as the name suggests is a fusion of time

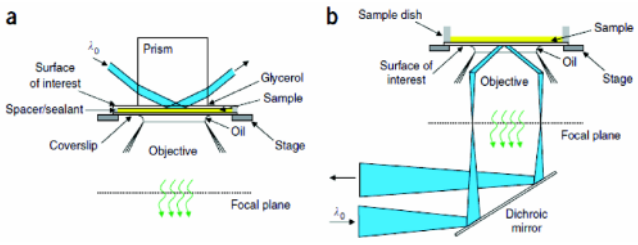

Figure 9: **TIR illumination modes (Adapted from Thompson *et al.*, 2007). (a) Through-prism mode with internal reflection being generated by focusing the laser beam through the prism onto the sample. Fluorescence generated from the sample from evanescent wave excitation is collected by the objective. (b) Through-objective mode; here the internal reflection is generated by focusing the beam through the periphery of a high numerical aperture objective and fluorescence form the sample is collected through the same objective**

correlated single photon counting (TCSPC) and FCS. The application of this concept was first shown by Enderglein and coworkers and the technique shows a lot of promise (Böhmer *et al.*, 2004). Some of the major advantages include: (i) separation of autocorrelation traces of a mixture of fluorophores provided these have distinctly different lifetimes, (ii) avoiding complications due to detector afterpulsing and/or spurious scattering or autofluorescent background that contribute to the overall correlation function (Kapusta *et al.*, 2007; Gregor *et al.*, 2007). Lifetime-weighted FCS, essentially an extension of FLCS, has also been shown to resolve heterogeneity of mixtures and at the same time allow the investigation of conformational fluctuations from nano- to milliseconds without having to deal with contributions from translational diffusion (Ishii *et al.*, 2010). Lamb and coworkers have also shown enhanced sensitivity in correlation measurements using the Time-gated FCS technique (Lamb *et al.*, 2000) that is very similar to FLCS.

2.6. *Scanning FCS*

Under normal conditions, FCS studies are point investigations i.e. photons are collected from samples moving in and out of the confocal volume due to diffusion from a single stationary point on the sample. However, for slow moving samples with very low diffusion coefficients, such point investigation gives rise to unwanted photobleaching thereby distorting the resultant autocorrelation trace. To circumvent this problem

the concept of scanning of either the sample or the laser beam (most common nowadays) was introduced leading to the development of scanning fluorescence correlation spectroscopy (SFCS) technique. In its earliest implementation for monitoring aggregation the sample was raster scanned while the laser beam was kept stationary (Petersen, 1986). Recent approaches in SFCS are based on the translation of a well-defined detection volume, that is, by moving the excitation beam across the sample, which is kept fixed (Petrásek *et al.*, 2008a; Digman *et al.*, 2005a). Depending upon the mobility of the species under investigation, the scan area can be reduced or enlarged to achieve the required temporal resolution. Alongwith the alleviation of photobleaching (by spending lesser amount of time on one definite spot) SFCS allows the user to measure fluorescence signals from multiple spots in a simultaneous manner. Moreover, the molecular brightness (η), an important parameter in FCS is increased (as compared to conventional single-point FCS) because of the increased number of independent sample volumes monitored. Indeed, the speed at which the laser excitation beam is scanned across the sample determines the temporal efficiency of the technique and hence can sometimes be its biggest drawback. Raster image correlation spectroscopy (RICS) developed by Gratton and coworkers has shown the capability to measure spatially resolved fluctuation dynamics in the microsecond-to-second range thus further extending the limits and extent of impact of SFCS (Digman *et al.*, 2005b). An excellent bottom-up approach involving instrumentation details can be found in the reference by Rossow *et al.* (2010). Confocal laser scanning microscopes are becoming increasingly common in research laboratories and are also being commercially manufactured by a number of companies (Table 1).

2.7. Other Variations

Winckler *et al.* have developed a novel and interesting method based on nonradiative excitation to achieve attoliter sized confocal volumes for FCS studies. The authors activated the cover glass surface with a thin film of PMMA doped with quantum dots that on excitation transferred energy nonradiatively via FRET to the diffusing Alexa 647 dyes in water (Winckler *et al.*, 2010). Since FRET provides a distance resolution of 1-10 nm, hence only those Alexa647 molecules that would be at a distance of the order of ~10 nm would be illuminated, thus providing a significant improvement in spatial resolution (**Fig. 10**). Martinez and coworkers using field enhancement effect by optical nanoantennas have also provided a means of reducing the volume for FCS measurements by at least 4 orders of magnitude as compared to the conventional one-photon FCS method (Estrada *et al.*, 2008). Apart from these recent endeavours at reducing sampling volume, Webb and coworkers (Levene *at el.*, 2003) have introduced apertures (30 nm) leading to zero-mode waveguides for FCS that have further reduced the volume to the order of few tens of zeptoliters (1zL = 10^{-21} L) (Leutenegger et al., 2006). Indeed a lot of phenomena in biology require micromolar concentrations which are at the limits of the standard confocal FCS (one-photon). Hence recent years as referred to in this section have shown increased attempts towards bringing about drastic reductions in excitation volumes such that reactions can be monitored at much higher concentrations (**Fig. 11**), as has been very elegantly reviewed by Wenger and Riegnault (Wenger *at al.*, 2010).

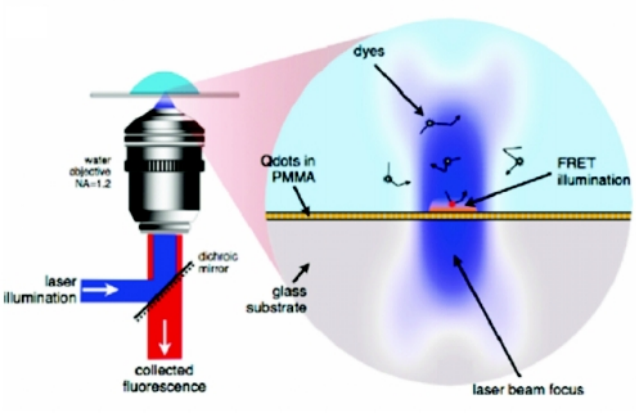

Figure 10: **Scheme of the approach based on nonradiative excitation induced reduction in probe volume. Illumination through FRET only occurs close to the activated surface thus leading to a dramatic reduction in excitation volume. (Adapted from Winckler *et al.*, 2010, copyright American Chemical Society)**

3. Applications

3.1. Protein Aggregation

FCS has been used quite extensively in analyzing the aggregation/polymerization characteristics of proteins with particular regards to the underlying mechanism and distribution of the involved oligomeric species. Aggregation of proteins has been a topic of great interest because of its direct link with a myriad of diseases (cognitive and neurodegenerative). For example, patients suffering from Alzheimer's are known to have plaque deposits in their brain formed from the aggregation of the amyloid beta (Aβ) peptide. Pitschke *et al*. provided one of the earliest studies using FCS to detect the presence of Aβ aggregates in the cerebrospinal fluid samples of Alzheimer's patients (Pitschke *et al*., 1999). Rigler and coworkers studied the oligomerisation of the amyloid beta ($A\beta_{1\text{-}40}$) peptide in absence and presence of potential inhibitors (Tjernberg *et al*.; 1999). The authors showed that the larger aggregates formed rapidly from monomers or dimers without significant population of the intermediate oligomers. Maiti and coworkers have also used FCS to probe Aβ aggregation and have shown the efficacy of using the MEMFCS fitting routine and its advantage over the normal fitting procedure for a process as heterogeneous as this (Sengupta *et al*., 2003). The heterogeneity of protein aggregation was further brought into focus by Gai and coworkers in their study of the polymerization and depolymerization of a-antitrypsin, the latter belonging to the serpin superfamily (Purkayastha *et al*., 2005; Chowdhury *et al*., 2007). The distribution of diffusion times obtained from the FCS measurements revealed the abrupt formation of longer oligomers from shorter ones (**Fig. 12**) with the lag time for the polymerization process showing a marked dependence on temperature (Purkayastha *et al*., 2005). Similarly, the depolymerization of preformed α-antitrypsin polymers using a set of four-residue peptides (obtained through computational design) was found to proceed through a combination of mechanisms that included the internal fragmentation of longer oligomers and sequential deletion of the shorter ones (Chowdhury *et al*., 2007). In a related study, the stabilizing and destabilizing property of

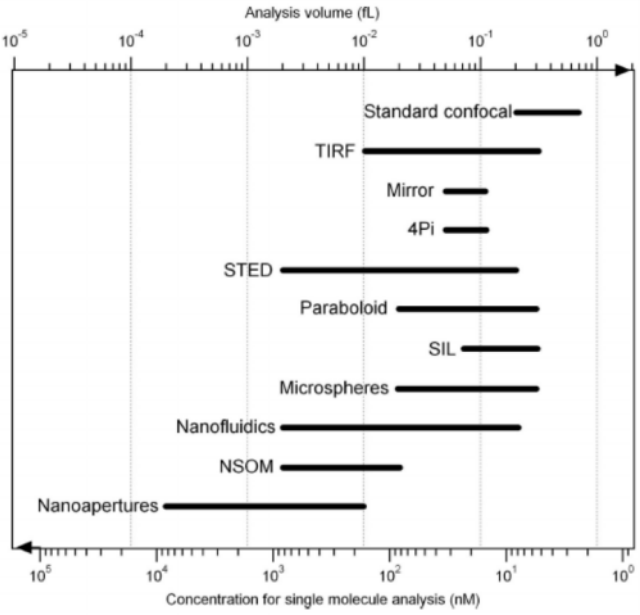

Figure 11: **A schematic comparing the range of analyses concentrations for different approaches ensuring the presence of single molecules in the excitation volume. (Adapted from Wenger *et al*., 2010)**

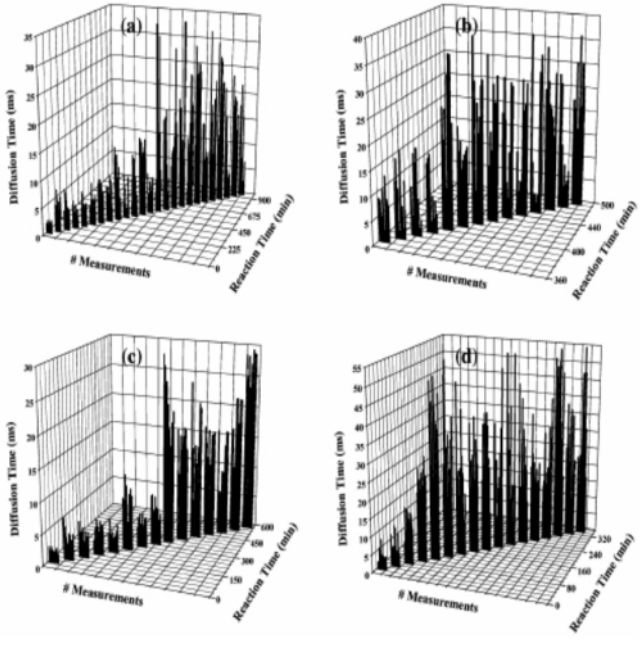

Figure 12: **Distribution of diffusion times of polymers of the protein a-antitrypsin as a function of incubation (reaction) time at different temperatures: (a) 45 °C (c) 50 °C and (d) 55 °C. Evident is the heterogeneity of the process along with the abrupt formation of longer polymers from shorter ones. A decrease in lag time of the polymers with increase in temperature is also observed. The distribution of diffusion times at 45 °C at the point of formation of the longer chain polymers is shown in (b). (Adapted from Purkayastha *et al*., 2005, copyright American Chemical Society)**

arginine as an osmolyte was used to study the effect on aggregation of the protein bovine serum albumin (BSA). The authors showed that arginine inhibited the accumulation of partially folded intermediates that can potentially be involved in the aggregation process (Ghosh *et al*., 2009). The tendency of monomeric polyglutamine molecules to form collapsed structures in solution has also been shown using FCS. The importance of this study lies in the fact that water being a poor solvent provides a generic driving force for polyglutamine aggregation, which is responsible for Huntington's disease (Crick *et al*., 2006). To avoid the need for conjugation of extrinsic fluorophores, the two-photon FCS approach has also been employed in recent past to monitor protein aggregation through the intrinsic tryptophan fluorescence of the protein barnase (Sahoo *et al*., 2009).

3.2. Protein Folding and Dynamics

3.2.1. Conformational Dynamics

Only of late have researchers realized the potential of FCS in revealing much needed dynamical information about proteins. In one of the first applications of this kind, Chattopadhyay *et al.* used two strategic cysteine mutations of the intestinal fatty acid binding protein, Val60Cys and Phe62Cys, to incorporate thiol reactive Fluorescein and Alexa chromophore (Chattopadhyay *et al*., 2002). Autocorrelation curves obtained from FCS measurements revealed the presence of a 35 ms relaxation component for the Val60Cys-Flu mutant, but was notably absent in case of the other mutant. This exponential component was attributed to the dynamic quenching of fluorescein by a nearby tryptophan (Trp-82) residue resulting from fast local conformational fluctuations that brought the two moieties (Trp and Flu) in close proximity. For the mutant Phe62Cys-Flu wherein the fluorophore was exposed, no such fast fluctuation was seen since the Trp was at too far a distance to show any possible quenching effects. Based on a similar concept, the authors also studied the fluctuation dynamics of denatured/unfolded IFABP using the double mutant (D59C/E107C). Both the cysteine residues were labeled by TMR-5 maleimide and the fluorescence fluctuation arising from the self-quenching of fluorescence of the TMR dyes was analyzed using FCS. Depending on the external conditions, conformational dynamics less than 10 ms arising from, according to the authors, transient formation and dissolution of ordered substructures were observed (Chattopadhyay *et al*., 2002). Indeed such unfolded chain dynamics can provide important insights into the energy landscape of the denatured state and hence its role in reaching the ultimate native ensemble. A similar microsecond conformational dynamics has also been observed in the unfolded state of yeast cytochrome c (Christian *et al.*, 2003). The authors in this case used the clever notion of monitoring energy transfer dynamics between Alexa-488 as the donor and the haem group of the protein itself as the acceptor. Thus variation in fluorescence observed from the Alexa dye was dependent on its distance from the haem and hence the conformational state of the protein. In other words, fluctuations in the fluorescence intensity were directly related to the fluctuations in the donor-acceptor distance in the denatured state of the protein. Neuweiler et al. used an elegant approach based on the photoinduced electron transfer (PET) mechanism to elucidate the folding mechanism of Trp-cage, a 20-residue protein (**Fig. 13**). Lysine residues in the peptide sequence were labeled with the oxazine dye MR121. Quenching of fluorescence of MR121 by the Trp residue gave rise to fluorescence intensity fluctuations that led to conformational dynamics in the microsecond to submicrosecond timescale as obtained by fitting the resultant autocorrelation traces (Neuweiler *et al*., 2005). Based on the collected data from the native protein and its mutant as a function of thermal, chemical and pH induced denaturation, the authors concluded that Trp-cage folding involved the presence of an intermediate, as opposed to the existing popular two-state model. This study further underscored the importance of preformed structure in the denatured state for efficient folding of the smallest available globular protein. FCS has also been used by Webb and coworkers to monitor fluctuations of the protein apomyoglobin across several distinguishable timescales (Chen *et al*., 2007). The origins of the time constants in the range of 3, 30, 100 and 200 μs were attributed to interconversions

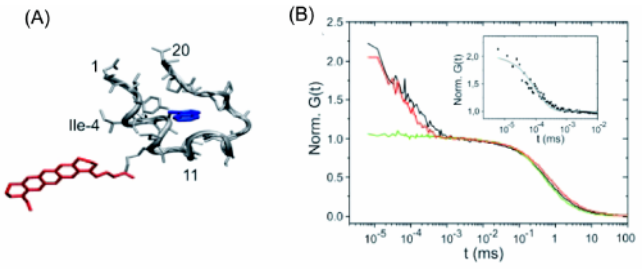

Figure 13: **(A) NMR Structure of modified Trp-cage protein. The MR121 dye is shown in red while the Tryptophan residue involved in PET with the dye is shown in blue. Depending on the conformation and associated dynamics PET occurs which is reflected as an additional component in the autocorrelation curve. (B) FCS curves showing additional components due to nanosecond relaxation kinetics (the inset zooms into the nanosecond relaxation kinetics and the corresponding exponential fit). The green curve is that of the mutant wherein the Trp was mutated and hence there was no PET therefore giving rise to no visible relaxation component in the nanosecond time scale. (Adapted from Neuweiler *et al.* (2005), copyright 2005 National Academy of Sciences, USA)**

between different conformational substates in the unfolded (U), intermediate (I) and the native (N) ensemble as a function of varying pH. Such a broad distribution of relaxation times reveals the inherent complexity of the folding/unfolding landscape of proteins and also reinforces the utility of FCS in extracting such valuable information. Fast conformational fluctuation dynamics have been observed by Deniz and coworkers in the prion determining domain NM, consisting of the amyloidogenic domain N and a solubilizing middle region M. The dynamics were in the range of 20–300 ns i.e. in the submicrosecond timescale and arose from the proximity of tyrosine residues that quenched the fluorescence of the dye Alexa-488 (Mukhopadhyay *et al.*, 2007). In a very recent study, Rogers *et al.* used the PET induced fluorescence fluctuation and local motions of a dye to probe the pH induced conformational dynamics of a truncated version of the influenza A M2 proton channel in presence and absence of drug (proton channel inhibitor) molecules (Rogers *et al.*, 2011).

3.2.2. Unfolding of Proteins through Diffusion

FCS has also been used to monitor the changing hydrodynamic radii of proteins during folding and unfolding transitions by tracking the respective diffusion times under the given set of experimental conditions. Frieden and coworkers provided an in-depth analysis of FCS measurements of unfolded IFABP in presence of varying concentrations of the commonly used chemical denaturant guanidine hydrochloride (Chattopadhyay *et al.*, 2005). As was shown in the paper, measurements in such denaturant solutions involve extreme care with regards to data analyses and interpretation. With increase in concentration of GdnHCl, both the viscosity and refractive index of the solution change. While viscosity results in an increase in observed diffusion times, changes in refractive index lead to a mismatch between that of the protein solution and immersion medium of the objective leading to aberration related artifacts. To correct for this aberration, variation of the correction collar settings of the objective was carried out by the authors. Unfolded proteins are generally considered as self-avoiding random coils and are thought to follow the Flory-statistics. According to Flory's law $R_G = R_0 N^{\nu}$, where R_G is the radius of gyration, R_0 is a constant determined by the persistence length of the polymer, N is the number of residues, and ν is a scaling exponent that depends on the quality of the solvent. The study of the denatured state(s) of IFABP showed that the protein typically follows random-coil statistics and the change in the diffusion times of the protein from its folded to the unfolded state matched well with the two-state thermal transition (as observed using CD) (Chattopadhyay *et al.*, 2005). That such detailed and sometimes complicated analyses for aberration correction are not always necessary was pointed out by Sherman et al. in their recent paper (Sherman *et al.*, 2008). The authors revealed that standardizing and calibrating the FCS spectrometer using the known diffusion coefficient of the dye rhodamine 6G can provide an accurate estimation of the changes brought about by variation in refractive index and viscosity of the protein solution. The authors further studied the coil to globule transition of two proteins, Protein L and Adenylate Kinase (AK) using the hydrodynamic radii values obtained from FCS. The two proteins showed markedly different behaviour with respect to the nature of expansion of their unfolded states in presence of GdnHCl. While protein L showed almost a continuous expansion even after ~5M GdnHCl, AK reached its maximally expanded

conformation just at ~3M. This observed difference is probably due to the specifics of the structures of the two proteins as proposed in that paper. The calculated hydrodynamic radii from the diffusion times of the unfolded proteins were also in good agreement with that proposed by Wilkins *et al.* based on NMR studies (Wilkins *et al.*, 1999). Gai and coworkers used the statistical nature of FCS to provide insights into the unfolding profile of an immunoglobulin (IgG) fragment, $F(ab')_2$ and an IgG binding protein, protein A. Apart from the fact that protein A is alpha helical while $F(ab')_2$ is predominantly composed of β-sheets, protein A also, unlike that of the IgG fragment (has 12 disulfide bonds), is devoid of any disulfide crosslinks. The GdnHCl induced denaturation profiles for the two proteins as measured were observed to be quite different from each other. Protein A expanded almost in a continuous fashion as expected from Flory's hypothesis. However, the IgG fragment exhibited an unusual behaviour wherein the diffusion time(s) went through a maximum at intermediate GdnHCl concentrations followed by a sudden decrease at higher concentrations of the denaturant (**Fig. 14**). The authors hypothesized that electrostatic repulsion was the dominant factor leading to the formation of such a highly expanded $F(ab')_2$ ensemble at intermediate GdnHCl concentrations. Addition of 2M NaCl to the highly expanded ensemble immediately led to a drastic compaction in size thus further supporting the fact that electrostatic repulsions can play a significant role in defining the molecular dimensions of denatured states. Another interesting aspect of this paper was the observed spread in diffusion times observed at any given condition and especially at the intermediate range of GdnHCl concentration for the IgG fragment. Not only did this reveal the heterogeneity of the expanded ensemble but also that the underlying reconfiguration times among different conformations were slower than their respective transit times through the confocal volume.

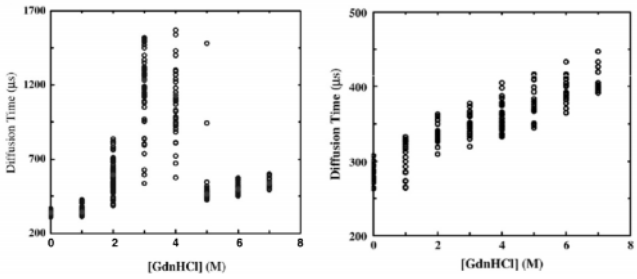

Figure 14: **Monitoring unfolding of proteins using FCS as a function of guanidium hydrochloride (GdnHCl) concentration (adapted from Guo *et al.*, 2008, copyright American Chemical Society). The left panel shows the diffusion times of the Alexa-labeled IgG fragment with the red dots showing the respective average values. The right panel shows the same for Protein A. The diffusion times have been corrected for viscosity as mentioned in the paper. Apart from the observed difference in the denaturation profiles (see text for explanation), one should also note the spread in diffusion values obtained from repetitive measurements indicating the presence of protein ensemble of varying molecular dimensions**

3.2.3. FCS-FRET Approach

Single molecule Förster resonance energy transfer studies often suffer from the disadvantage of not being able to resolve fast dynamics due to the typically large bin times (~ 1ms) used for collecting photons from the donor and acceptor moieties. Schuler and coworkers used FRET in combination with FCS to shed light on nanosecond to microsecond dynamics of the cold shock protein from *Thermotoga maritima* (Nettels *et al.*, 2007; Nettels *et al.*, 2008) By using the start-stop mode of their photon counter (PicoHarp 300 from PicoQuant) along with conventional FCS, the authors could go down to even picosecond timescales thus providing ample scope to probe nanosecond relaxation dynamics of unfolded proteins or those folding on the ultrafast timescale (Nettels *et al.*, 2008). Using this configuration it was observed that the dynamics of the Csp protein (considered to be a two-state folder) in its unfolded state were dominated by diffusive chain reconfiguration in the range of tens of nanoseconds. Levitus and his group have also used the FCS-FRET approach albeit from a different viewpoint. Since extracting conformational dynamics from FCS experiments can often be troublesome (Gurunathan *et al.*, 2010), the authors used the correlation from fluctuations in the FRET signal to separate the kinetic and translational diffusion contributions by analyzing ratios of auto- and cross-correlation functions of the donor(acceptor) only and donor-acceptor, respectively (Torres *et al.*, 2007). The FCS-FRET approach has also been applied to the

study of the dynamics of calmodulin wherein cross-correlation of the donor and acceptor moieties revealed the presence of protein motion on a number of timescales (Slaughter *et al.*).

3.2.4. Photodynamics of Fluorescent Proteins

With the advent of a variety of fluorescent proteins and their increasing usage as noninvasive fluorescent markers, studying their intrinsic fluorescent dynamics becomes necessary. Haupts et al. used FCS to probe fast equilibrium fluctuations resulting from pH dependent processes of mutants of the Green Fluorescent Protein (**Fig. 15**). The autocorrelation traces show the distinct presence of additional chemical relaxation along with the fluctuation arising from the diffusion of the protein molecules into and out of the confocal volume (Haupts *et al.*, 1998). Moreover, the relaxation components were significantly affected by the pH of the medium with decreasing pH bringing about an increase in the amplitude of fluctuation due to chemical relaxation. Rigler and coworkers revealed similar dynamic process of GFP mutant proteins using FCS and also measured the photostabilities of the proteins by varying the excitation intensities of the source laser (Widengren *et al.*, 1999). Correlation measurements on yellow-shifted GFP mutants not only showed intensity-dependent flickering at high pH but also provided the evidence of two distinct dark states. Using a combined time-resolved fluorescence and FCS approach, Heikal and coworkers explained the pH dependence of fluorescence flickering based on increased segmental mobility that resulted in structural changes of the β-barrel (GFPs) at low pH (Liu *et al.*, 2006) DsRed, the red emitting counterpart of GFP, also shows strong evidence of light induced flickering similar to the yellow-shifted mutants. In addition, the FCS studies further revealed that DsRed has at least three interconvertible states with one of these being fluorescent (Malvezzi-Campeggi *et al.*, 2001; Schenk *at al.*, 2004; Hendrix *et al.*, 2008, Seward *et al.*, 2009). A comprehensive reorganization of the chromophore of the protein Kaede from green to red on photoconversion has also been studied using FCS (Dittrich *et al.* 2005). Huser and corworkers used FCS to investigate the hydrodynamics and photophysical properties of PR1, an intensely red biliprotein variant of the truncated cyanobacterial phytochrome 1. The study revealed that not only did PR1 have excellent fluorescent brightness making it a good candidate for fluorescence tagging but also showed enhanced emission characteristics when forming a heterodimer with apoCph1Δ (Miller *et al.*, 2006).

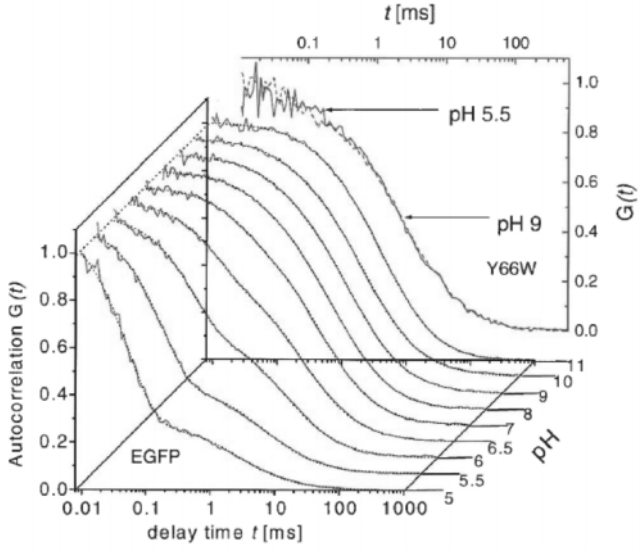

Figure 15: **FCS correlation curves for the fluorescence fluctuations of the EGFP protein at different pH values (adapted from Haupts *et al.* (1998), copyright 1998 National Academy of Sciences, USA). At high pH, the correlation function is dominated by diffusional process. With decrease of pH however, a fast chemical relaxation is observed (because of proton exchange) which increases in amplitude and rate as the pH is lowered. The *inset* (in red) shows the correlations curves at pH values of 9 (solid line) and 5.5 (broken line) for the GFP-Y66W mutant. Both these curves are almost superimposable with each other showing the absence of fast flickering since the chromophore lacks a protonatable hydroxyl group**

3.3. In Membranes

One of the areas where FCS has been used most extensively and effectively is the study of membranes. Interest in this specific area stems from the fact that biological membranes are highly dynamic in nature and is involved in a lot of cellular processes and signaling pathways (Macháň *et al.*, 2010, 2011). Also these membranes are known to be highly heterogeneous and composed of nanodomains known as lipid rafts that might serve as specific sites for sorting of cells (Kahya *et al.*, 2003). In addition the lateral diffusion of molecules on these membranes is also

vital for many cellular activities. Realistic modeling of biological membranes is not easy. Hence planar lipid membranes like supported bilayers or giant unilamellar vesicles have widely been used as models for cellular membranes. GUVs are generally considered to be better models since these are free-standing as opposed to the SLBs which form via adsorption and fusion of lipid vesicles on hydrophilic surfaces such as glass or mica. FCS on GUVs carried out by Feigenson and coworkers revealed the existence of fluid, spatially ordered and high cholesterol content phases by monitoring the diffusion of the fluoresecent probe DiI-C_{20} (1,19-dieicosanyl-3,3,39,39-tetramethylindocarbocyanine perchlorate) (Korlach *et al.*, 1999). For single photon FCS set-up, the optimum concentration ratio of labeled lipids to non-labeled ones has been found to be of the order of ~10^{-5} for studying lipid diffusion in membranes (Macháň *et al.*, 2010). FCS studies have also helped reveal the key role played by cholesterol in tuning lipid dynamics in GUV membranes (Kahya *et al.*, 2003). It has recently been demonstrated that FCS has the potential to be a valuable tool in the study of lipid raft associations, both in model membranes exhibiting domains and in cell membranes (Bacai *et al.*, 2004; Wawrezinieck *et al.*, 2005). Hof and coworkers have introduced the Z-scan approach in monitoring membrane dynamics and diffusion, wherein the FCS traces are collected as a function of different positions (step size of 100 or 200 nm) of the sample in the axial direction. Membrane diffusion in many cases has also been found to be anomalous in nature. Moreover, diffusion of a pH low insertion peptide (pHLIP) in membranes was shown to very much dependent on the conformational properties of the peptide thus giving rise to a wide spread in the recovered diffusion times (Guo *et al.*, 2010). That FCS has been instrumental in revealing significant new details about membrane diffusion and dynamics can be realized from the vast number of studies that have already been carried out (see excellent reviews by Chen *et al.*, 2006; Macháň *et al.*, 2010, 2011).

3.4. Anomalous Diffusion

Diffusion in fractal surfaces has often been observed to be anomalous in nature (Havlin *et al.*, 1987). The word anomalous implies deviation of diffusive motion from the normally encountered Brownian movement. Brownian motion is characterized by the simple random walk model wherein the mean squared displacement of a diffusing particle is proportional to time and is given by:

$$\left\langle r^2(t)\right\rangle = 2nDt \tag{11}$$

where D is the time-independent diffusion coefficient, t is the time and n represents the dimensionality of the system. However for systems exhibiting anomalous diffusion, the aforesaid linearity of MSD with time is not maintained (Hellman *et al.*, 2011). Instead it exhibits a power-law scaling as follows (Wu *et al.*, 2008):

$$\left\langle r^2(t)\right\rangle = \Gamma t^{\alpha} \tag{12}$$

where Γ is the transport factor (Wu *et al.*, 2008; Baumann *et al.*, 2010). If the exponent α is less than 1, the motion is referred to as subdiffusive while for a greater than 1, the tracer particle is said to be in the superdiffusive regime. Using an anomalous diffusion propagator, Wu and Berland proposed an alternative expression for the diffusion time τ_D (obtained from the FCS traces) as follows (Wu *et al.*, 2008):

$$\tau_D = \left(\frac{\alpha \omega_{xy}^2}{4mD_{inst}(\tau)} \right) \tag{13}$$

where m represents the type of excitation, that is, one photon (m = 1) or two-photon (m = 2), ω_{xy} is the radial beam waist and $D_{\text{inst}}(t)$ is the instantaneous diffusion coefficient given by the following expression:

$$D_{inst}(t) = \frac{\alpha}{2n} \Gamma t^{\alpha-1} \tag{14}$$

with α and n having the same meanings as in equations 11 and 12. Weiss *et al*. have used the subdiffusive diffusion behaviour as a measure of the extent of crowding present in the cytoplasm (Weiss *et al.*, 2004). The viscoelastic properties of different cells have also been monitored using FCS wherein the anomaly in diffusion was observed to decrease as a function of increased

cellular osmotic stress (Guigas *et al.*, 2007). Furthermore, in presence of high concentrations of polymers, protein motion has also been found to be subdiffusive (Banks *et al.*, 2005) thus further confirming previous observations of anomalous diffusion in the cytoplasm (Feder *et al.*, 1996; Wachsmuth *et al.* 2000). Cellular interior has often been likened to fractal domains (Codling *et al.*, 2008; Losa, 2009; Mashiah *et al.*, 2008) with the diffusion lengthscales of molecules differing from the normal Brownian type because of the presence of obstacles/hindrances (either mobile or immobile). Indeed recent years have seen increased interest in studying the nature of diffusion inside cells (Fritsch *et al.*, 2010) and in crowded media (Sanabria *et al.*, 2007; Guigas *et al.*, 2007; Goins *et al.*, 2008; Dix *et al.*, 2008; Szymanski *et al.*, 2009) since consequences of subdiffusive motion can be quite significant, in particular, with respect to molecular recognition (Savageau, 1993) and enzyme kinetics (Malchus *et al.* 2010). Sauer and coworkers have hypothesized based on unfolded peptide dynamics in crowded environment that hindered diffusion might not be able to deter the early formation of structural elements (Neuweiler et al., 2007). Examples of superdiffusive motion can often be found in case of directed flow of particles. One such case has been shown by Guo *et al.* wherein the superdiffusion was proposed to be due to the well-ordered packing of lipid molecules in the lipid tubules hence giving rise to directed flow of the dye molecules (Guo *et al.*, 2007). Active transport of GFP through plastid tubules also gave rise to correlation traces that had to be fitted using both components from diffusion and directed flow (Köhler *et al.*, 2000).

3.5. Nucleic Acids

Rigler and his group investigated the hybridization of fluorescently tagged deoxyribonucleotides with complementary DNA templates using FCS (Kinjo *et al.*, 1995) and also monitored the progress of PCR reactions using the same technique (Björling *et al.*, 1998). FCS studies have revealed the existence of DNA breathing dynamics over a range of timescales (Altan-Bonnet *et al.*, 2003). Van Orden and coworkers proposed a three-state reaction mechanism for formation of DNA hairpin using multiparameter FCS. Their study revealed the presence of intermediate conformations that could play an important role in biological reactions using RNA and DNA. Conformational transitions of single stranded DNA have also been monitored using the PET-FCS technique based on the quenching of the oxazine dye MR-121 by intrinsic guanosine residues (Kim *et al.* 2006; Li *et al.*, 2011). The rate limiting step of DNA folding was found to be dominated by interactions between the nucleotides of the loop and the stem (Kim *et al.* 2006). A similar approach has also been employed by Kaji et al. to probe dynamics of ssDNA over a substantial time range of nanoseconds to the submillisecond regime (Kaji *et al.*, 2009). A combined FCS-FRET approach was recently used to probe the base-by-base dynamics of double stranded DNA wherein the terminal ends of the complementary strands were labeled by FRET pairs.

4. FCS Fluorophores

Any discussion on FCS will be incomplete without the mention of the fluorescent reporters (either intrinsic or extrinsic) and hence in this section I have provided a brief overview of the same that are being used regularly for FCS studies. A number of practical aspects need to be considered before selection of a specific reporter. An obvious consideration is that the fluorophores should be able to absorb the laser excitation wavelength. The brightness of a dye molecule is an extremely important parameter on which the statistics of FCS measurements are mainly dependent. High brightness is typically ensured by a combination of high extinction coefficient, high quantum yield, low intersystem crossing and relatively high photostability (Krichevsky *et al.*, 2002; Mütze *et al.*, 2011). Nowadays the Alexa dyes developed by molecular probes (USA), the Atto dyes manufactured by Attotec (Germany) and the HiLite Fluor dyes patented by Anaspec (USA) are the best available not only with regard to the brightness criteria but also because they manage to cover a wide range of the visible spectrum. Photobleaching of fluorophores under high excitation internsities or because of extended illumination in case of slow moving particles can pose considerable problems in FCS data analyses. Dissolved molecular oxygen has been known to

be the main culprit in bringing about irreversible photodamage of the reporters because of photo-oxidation and hence enzymatic oxygen scavenging systems like glucose oxidase and catalase are sometimes added to the reaction mixture to minimize photodestruction (Mütze *et al.*, 2011). Along with these external fluorophores, many variants of fluorescent proteins are also being used nowadays as markers. GFP exhibits the maximum brightness and photostability but also shows pH dependent fluorescence fluctuations (as mentioned above). The other variants like red fluorescent protein has reduced brightness though with recent efforts better options have been found (Mütze *et al.*, 2011).

5. Conclusions

The scope of fluorescence correlation spectroscopy in present day research is increasing quite rapidly. The most appealing characteristic of this technique is its versatility (combined with its non-invasiveness) as can be made out from the wide spectrum of problems that FCS is able to address. Recent innovations in instrumentation to bring about reduction in excitation volume have further improved the utility of this analytical method. Furthermore, its application to biology and bio-systems has added a new dimension to its capability not only as a single molecule technique but also as a method that can be used to characterize fast dynamics, the latter often playing significant roles in many cellular processes. While this review has tried to point out the salient features of FCS and give readers a perspective of the range of scientific queries that can be tackled, I am sure there are a few that have been left out unintentionally for which I would like to duly apologize.

Acknowledgements

PKC thanks Indian Institute of Technology Delhi for providing the necessary infrastructure and DST, Government of India for financial support under the Fast Track Scheme for Young Scientists.

Abbreviations

FCS, fluorescence correlation spectroscopy; pM, picomolar; nM, nanomolar; FCCS, fluorescence cross correlation spectroscopy; PCH, photon counting histogram; FIDA, fluorescence intensity distribution analysis; APD, avalanche photodiodes; NSOM, near-field optical scanning microscopy (NSOM); NIR, near-IR; STED, stimulated emission depletion; FFS, fluorescence fluctuation spectroscopy; TIRFM, total internal reflection microscopy; FLCS, fluorescence lifetime correlation spectroscopy (FLCS); TCSPC, time correlated single photon counting; SFCS, scanning fluorescence correlation spectroscopy; Ab, amyloid beta; IFABP, intestinal fatty acid binding protein; Flu, fluorescein; PET, photoinduced electron transfer; GdnHCl, guanidine hydrochloride; R6G, rhodamine 6G; AK, adenylate kinase; FRET, Förster resonance energy transfer; Csp, cold shock protein; GFP, Green Fluorescent Protein; PR1, Phytofluor 1; Cph1D, truncated cyanobacterial phytochrome 1; SLBs, supported bilayers (SLBs); GUVs, giant unilamellar vesicles; pHLIP, pH low insertion peptide; MSD, mean squared displacement; PCR, polymerase chain reaction; ssDNA, single stranded DNA.

References

[1] Anastasia, L., Ingo, G., Christina, S., Markus, M. and Enderlein, J. (2010), Measuring rotational diffusion of macromolecules by fluorescence correlation spectroscopy. Photochem. *Photobiol. Sci.* **9**, 627-636.

[2] Aragon, S. R. and Pecora, R. (1975), Fluorescence correlation and Brownian rotational diffusion. *Biopolymers* **14**, 119-138.

[3] Altan-Bonnet, G., Libchaber, A. and Krichevsky, O. (2003), Bubble Dynamics in Double-Stranded DNA. *Phys. Rev. Lett.* **90**, 138101(1-4).

[4] Bacia, K. and Schwille, P. (2003), A dynamic view of cellular processes by in vivo fluorescence auto- and cross-correlation spectroscopy. *Methods* **29**, 74-85.

[5] Bacia, K., Kim, S.A. and Schwille, P. (2006), Fluorescence cross-correlation spectroscopy in living cells. *Nature Methods*, **3**, 83-89.

[6] Bacia, K., Scherfeld, D., Kahya, N. and Schwille, P. (2004), Fluorescence correlation spectroscopy relates rafts in model and native membranes *Biophys. J.* **87**, 1034–1043.

[7] Banks, D. S. and Fradin, C. (2005), Anomalous diffusion of proteins due to molecular crowding. *Biophys. J.* **89**, 2960-2971.

[8] Barcellona, M. L., Gammon, S. Hazlett, T., Digman, M. A. and Gratton, E. (2004), Polarized fluorescence correlation spectroscopy of DNA-DAPI complexes. *Microscop. Res. Tech.* **65**, 205–217.

[9] Baumann, G., Place, R. F., Földes-Papp, Z. (2010), Meaningful interpretation of subdiffusive measurements in living cells (crowded environment) by fluorescence fluctuation microscopy. *Current Pharm. Biotech.* **11**, 527-543.

[10] Berland, K. M., So, P. T. and Gratton E. (1995), Two-photon fluorescence correlation spectroscopy: method and application to the intracellular environment. *Biophys. J.* **68**, 694-701.

[11] Björling, S., Kinjo, M., Foldes-Papp, Z., Hagman, E., Thyberg, P. and Rigler, R. (1998), Fluorescence correlation spectroscopy of enzymatic DNA polymerization. *Biochemistry*, **37**, 12971-12978.

[12] Böhmer, M., Wahl, M., Rahn, H-J., Erdmann, R. and Enderlein, J. (2002), Time-resolved fluorescence correlation spectroscopy. *Chem. Phys. Lett.* **353**(5–6), 439–445.

[13] Chattopadhyay, K., Saffarian, S., Elson, E. L. and Frieden, C. (2002), Measurement of microsecond dynamic motion in the intestinal fatty acid binding protein by using fluorescence correlation spectroscopy. *Proc. Natl. Acad. Sci. U.S.A.* **99**, 14171-14176.

[14] Chattopadhyay, K., Elson, E. L. and Frieden, C. (2005), The kinetics of conformational fluctuations in an unfolded protein measured by fluorescence methods. *Proc. Natl. Acad. Sci. U.S.A.* **102**, 2385-2389.

[15] Chattopadhyay, K., Saffarian, S., Elson, E. L. and Frieden, C. (2005), Measuring unfolding of proteins in the presence of denaturant using fluorescence correlation spectroscopy. *Biophys. J.* **88**, 1413-1422.

[16] Chen, H, Rhoades, E, Butler, J. S., Loh, S. N. and Webb, W. W. (2007), Dynamics of equilibrium structural fluctuations of apomyoglobin measured by fluorescence correlation spectroscopy. *Proc. Natl. Acad. Sci. U.S.A.* **104**, 10459-10464.

[17] Chen, Y., Lagerholm, B. C., Yang, B. and Jacobson, K. (2006), Methods to measure the lateral diffusion of membrane lipids and proteins. *Methods.* **39**, 147-153.

[18] Chen, Y., Muller, J. D., So, P. T. C. and Gratton, E. (1999), The photon counting histogram in fluorescence fluctuation spectroscopy. *Biophys. J.* **77**, 553-567.

[19] Xudong Chen, Yan Zhou, Peng Qu, and Xin Sheng Zhao. (2008), Base-by-Base dynamics in DNA hybridization probed by fluorescence correlation spectroscopy. *J. Am. Chem. Soc.* **130**, 16947-16952.

[20] Chowdhury, P., Wang, W., Lavender, S., Bunagan, M. R., Klemke, J. W., Tang, J., Saven, J. G., Cooperman, B. S. and Gai, F. (2007), Fluorescence correlation spectroscopic study of serpin depolymerization by computationally designed peptides. *J. Mol. Biol.* **369**, 462-473.

[21] Christian, R., Lars, J. E. and Földes-Papp, Z. (2003), Microsecond structural fluctuations in denatured cytochrome c and the mechanism of rapid chain contraction. *J. Phys. Cond. Matt.* **15**, S1725–S1735.

[22] Codling, E. A., Plank, M. J. and Benhamou S. (2008), Random walk models in biology. *J. Royal Soc. Int.* **5**, 813-834.

[23] Crick, S. L., Jayaraman, M., Frieden, C., Wetzel, R. and Pappu, R. V. (2006), Fluorescence correlation spectroscopy shows that monomeric polyglutamine molecules form collapsed structures in aqueous solutions. *Proc. Natl. Acad. Sci.* **103**, 16764-16769.

[24] Davis, L. M. and Shen, G. (2006), Accounting for triplet and saturation effects in FCS measurements. *Curr. Op. Biotech.* **7**, 287-301.

[25] de Lange, F., Cambi, A., Huijbens, R., de Bakker, B., Rensen, W., Garcia-Parajo, M., van Hulst, N. and Fiador, C. G. (2001), Cell biology beyond the diffraction limit: near-field scanning optical microscopy. *J. Cell Sci.* **114**, 4153-4160.

[26] Digman, M. A., Brown, C. M., Sengupta, P., Wiseman, P. W., Horwitz, A. R. and Gratton, E. (2005b), Measuring fast dynamics in solutions and cells with a laser scanning microscope. *Biophys. J.* **89**, 1317-1327.

[27] Digman, M. A., Sengupta, P., Wiseman, P. W., Brown, C. M., Horwitz, A. R. and Gratton, E. (2005a), Fluctuation correlation spectroscopy with a laser-scanning microscope: exploiting the hidden time structure. *Biophys. J.* **88**, L33–L36.

[28] Dittrich, P. S., Schäfer, S. P. and Schwille, P. (2005), Characterization of the photoconversion on reaction of the fluorescent protein Kaede on the single-molecule level. *Biophys. J.* **89**, 3446-3455.

[29] Dix, J. A. and Verkman, A. S. (2008), Crowding effects on diffusion in solutions and cells. *Annu. Rev. Biophys.* **37**, 247-263.

[30] Eggeling, C., Ringemann, C., Medda, R., Schwarzmann, G., Sandhoff, K., Polyakova, S., Belov, V. N., Hein, B., von Middendorff, C., Schönle, A. and Hell, S. W. (2009), Direct observation of the nanoscale dynamics of membrane lipids in a living cell. *Nature*, **457**, 1159-1162.

[31] Ehrenberg, M. and Rigler, R. (1974), Rotational brownian motion and fluorescence intensity fluctuations. *Chem. Phys.* 4, 390-401.

[32] Ehrenberg, M., and Rigler, R. (1976), Fluorescence correlation spectroscopy applied to rotational diffusion of macromolecules. *Quart. Rev. Biophys.* **9**, 69-81.

[33] Elson, E. L. (2001), Fluorescence correlation spectroscopy measures molecular transport in cells. *Traffic* **2**, 789-796.

[34] Elson, E. L. and Magde, D. (1974), Fluorescence correlation spectroscopy: I. Conceptual basis and theory. *Biopolymers* **13**, 1-27.

[35] Estrada, L. C., Aramendía, P. F. and Martínez, O. E. (2008), 10000 times volume reduction for fluorescence correlation spectroscopy using nano-antennas. *Opt. Exp.* **16**, 20597-20602.

[36] Feder, T. J., Brust-Mascher, I., Slattery, J. P., Baird, B. and Webb, W. W. (1996), Constrained diffusion or immobile fraction on cell surfaces: a new interpretation. *Biophys. J.* **89**, 2960-2971.

[37] Földes-Papp, Z. (2006), What it means to measure a single molecule in a solution by fluorescence fluctuation spectroscopy. *Exp. Mol. Pathol.* **80**, 209–218.

[38] Földes-Papp, Z. (2007), 'True' single-molecule molecule observations by fluorescence correlation spectroscopy and two-color fluorescence cross-correlation spectroscopy. *Exp. Mol. Pathol.* **82**, 147–155.

[39] Fritsch, C. C. and Langowski, J. (2010), Anomalous diffusion in the interphase cell nucleus: the effect of spatial correlations of chromatin. *J. Chem. Phys.* **133**, 025101.

[40] Ghosh R., Sharma S., Chattopadhyay K. (2009), Effect of arginine on protein aggregation studied by fluorescence correlation spectroscopy and other biophysical methods. *Biochemistry* **48**, 1135-1143.

[41] Goins, A. B., Sanabria, H. and Waxham, M. N. (2008), Macromolecular crowding and size effects on probe microviscosity. *Biophys. J.* **95**, 5362-5373.

[42] Gösch, M. and Rigler, M. (2005), Fluorescence correlation spectroscopy of molecular motions and kinetics. *Adv. Drug Deliv. Rev.* **57**, 179-190.

[43] Gösch, M., Serov, A., Anhut, T., Lasser, T., Rochas, A., Besse, P.A., Popovic, R.S., Blom, H. and Rigler, R. (2004). Parallel single molecule detection with a fully integrated single-photon 2x2 CMOS detector array. *J Biomed. Opt.* **9**, 913-921.

[44] Gregor, I. and Enderlein, J. (2007), Time-resolved methods in biophysics. 3. Fluorescence lifetime correlation spectroscopy. Photochem. *Photobiol. Sci.* **6**, 13-18.

[45] Guigas G., Kalla C., Weiss M. (2007), Probing the nanoscale viscoelasticity of intracellular fluids in living cells. *Biophys. J.* **93**, 316-323.

[46] Guigas, G., Kalla, C. and Weiss M. (2007), The degree of macromolecular crowding in the cytoplasm and nucleoplasm of mammalian cells is conserved. *FEBS Lett.* **581**, 5094-5098.

[47] Guo, L. and Gai, F. (2010), Heterogeneous Diffusion of a Membrane-Bound pHLIP Peptide. *Biophys. J.* **98**, 2914-2922.

[48] Guo, L., Chowdhury, P., Fang, J. and Gai, F. (2007), Heterogeneous and anomalous diffusion inside lipid tubules. *J. Phys. Chem. B*, **111**, 14244-14249.

[49] Guo, L., Chowdhury, P., Glasscock, J. M. and Gai, F. (2008), Denaturant-induced expansion and compaction of a multi-domain protein: IgG. *J. Mol. Biol.* **384**, 1029-1036.

[50] Gurunathan K., Levitus M. (2010), FRET fluctuation spectroscopy of diffusing biopolymers: contributions of conformational dynamics and translational diffusion. *J. Phys. Chem. B*, **114**, 980-986.

[51] Haupts, U., Maiti, S., Schwille, P. and Webb, W. W. (1998), Dynamics of fluorescence fluctuations in green fluorescent protein observed by fluorescence correlation spectroscopy. *Proc. Natl. Acad. Sci. U.S.A.* **95**, 13575-13578.

[52] Haustein, E. and Schwille, P. (2003), Ultrasensitive investigations of biological systems by fluorescence correlation spectroscopy. *Methods* **29**, 153-166.

[53] Haustein, E. and Schwille, P. (2007), Fluorescence correlation spectroscopy: Novel variations of an established technique. Annu. Rev. Biophys. *Biomol. Str.* **36**, 151-169.

[54] Havlin, S. and Ben-Avraham, D. (1987), Diffusion in disordered media. *Advances in Physics* **51**: 187-292.

[55] Hell, S. W. (2007), Far-field optical nanoscopy. *Science* **316**, 1153-1158.

[56] Hellmann, M., Klafter, J., Heermann, D. W. and Weiss, M. (2011), Challenges in determining anomalous diffusion in crowded fluids. *J. Phys. Cond. Matt.* **23**, 234113.

[57] Helmchen F., Denk W. (2005), Deep tissue two-photon microscopy. *Nature Methods.* **2**, 932-940.

[58] Hendrix J., Flors C., Dedecker P., Hofkens J. and Y. Engelborghs. (2008), Dark states in monomeric red fluorescent proteins studied by fluorescence correlation and single molecule spectroscopy. *Biophys. J.* **94**, 4103-4113.

[59] Hess, S. T. and Webb, W. W. (2002), Focal Volume Optics and Experimental Artifacts in Confocal Fluorescence Correlation Spectroscopy. *Biophys. J.* **83**, 2300-2317.

[60] Hess, S. T., Huang, S. H., Heikal, A. A. and Webb, W. W. (2002), Biological and chemical applications of fluorescence correlation spectroscopy. *Biochemistry* **41**, 697-705.

[61] Hwang, L. C., Gosch, M., Lasser, T. and Wohland, T. (2006), Simultaneous multicolor fluorescence cross-correlation spectroscopy to detect higher order molecular interactions using single wavelength laser excitation. *Biophys. J.* **91**, 715–727.

[62] Ishii K., Tahara T. (2010), Resolving inhomogeneity using lifetime-weighted fluorescence correlation spectroscopy. *J. Phys. Chem. B*, **114**, 12383-12391.

[63] Jung, J., Ihly, R., Scott, E., Yu, M. and Van Orden, A. (2008), Probing the Complete Folding Trajectory of a DNA Hairpin Using Dual Beam Fluorescence Fluctuation Spectroscopy. *J. Phys. Chem. B*, **112**, 127-133.

[64] Jung, J. and Van Orden, A. (2006), A three-State mechanism for DNA hairpin folding characterized by multiparameter fluorescence fluctuation spectroscopy. *J. Am. Chem. Soc.* **128**, 1240-1249.

[65] Kahya, N. Scherfeld, D. Bacia, K. Poolman, B. and Schwille, P. (2003), Probing Lipid Mobility of Raft-exhibiting Model Membranes by Fluorescence Correlation Spectroscopy. *J. Biol. Chem.* **278**, 28109-28115.

[66] Kaji, T., Ito, S., Iwai, S. and Miyasaka, M. (2009), Nanosecond to submillisecond dynamics in dye-labeled single-stranded DNA, as revealed by ensemble measurements and photon statistics at single-molecule level. *J. Phys. Chem. B,* **113**, 13917-13925.

[67] Kapusta, P., Wahl, M., Benda, A., Hof, M. and Enderlein, J. (2007), Fluorescence lifetime correlation spectroscopy. *J. Fluor.* **17**, 43-48.

[68] Kask, P., Palo, K., Ullmann, D. and Gall, K. (1999), Fluorescence-intensity distribution analysis and its application in biomolecular detection technology. *Proc. Natl. Acad. Sci. U.S.A.* **96**, 13756-13761.

[69] Kask, P., Piksarv, P., Mets, U. Pooga, M. and Lippmaa, E. (1987), Fluorescence correlation spectroscopy in the nanosecond time range: Rotational diffusion of bovine carbonic anhydrase B. Eur. *Biophys. J.* **14**, 257-261.

[70] Kask, P., Piksarv, P., Pooga, M., Mets, U. and Lippmaa, E. (1988), Separation of the rotational contribution in fluorescence correlation experiments. *Biophys. J.* **55**, 213–220.

[71] Kastrup, L., Blom, H., Eggeling, C. and Hell, S. W. (2005), Fluorescence fluctuation spectroscopy in subdiffraction focal volumes. *Phys. Rev. Lett.* **594**, 178104.

[72] Kim, J., Doose, S., Neuweiler, H. and Sauer, M. (2006), The initial step of DNA hairpin folding: a kinetic analysis using fluorescence correlation spectroscopy. *Nucleic Acids Res.* **34**, 2516-2527.

[73] Kim, S.A. and Schwille, P. (2003), Intracellular applications of fluorescence correlation spectroscopy: prospects for neuroscience. *Curr. Op. Neurobiol.* **13**, 583-590.

[74] Kim, S. A., Heinze, G. K. and Schwille, P. (2007), Fluorescence correlation spectroscopy in living cells. *Nature Methods*, **4**, 963-973.

[75] Kinjo, M. and Rigler, R. (1995), Ultrasensitive hybridization analysis using fluorescence correlation spectroscopy. *Nucleic Acids Res.* **23**, 1795-1799.

[76] Köhler, R. H., Schwille, P., Webb, W. W., and Hanson, M. (2000), Active transport of GFP through plastid tubules quantified by fluorescence correlation spectroscopy. *J. Cell Sci.* **113**, 392–393.

[77] Korlach, J. Schwille, P. Webb, W.W. and Feigenson, G. W. (1999), Characterization of lipid bilayer phases by confocal microscopy and fluorescence correlation spectroscopy, *Proc. Natl. Acad. Sci. USA*, **96**, 8461–8466.

[78] Krichevsky, O. and Bonnet, G. (2002), Fluorescence correlation spectroscopy: the technique and its applications. *Rep. Prog. Phys.* **65**, 251-297.

[79] Lamb, D. C., Schenk, A., Röcker, C., Scalfi-Happ, C. and Nienhaus, G. U. (2000), Sensitivity enhancement in fluorescence correlation spectroscopy of multiple species using time-gated detection. *Biophys. J.* **79**, 1129-1138.

[80] Leutenegger, M., Gösch, M., Perentes, A., Hoffmann, P., Martin, O.J.F. and Lasser, T. (2006), Confining the sampling volume for Fluorescence Correlation Spectroscopy using a sub-wavelength sized aperture. *Opt. Exp.* **14**, 956–969.

[81] Levene, M. J., Korlach, J., Turner, S. W., Foquet, M., Craighead, H. G. and Webb, W. W. (2003), Zero-mode waveguides for single-molecule analysis at high concentrations. *Science*, **299**, 682–686.

[82] Lewis, A., Kuttner, Y. Y., Dekhter, R., Polhan, M. (2007), Fluorescence Correlation Spectroscopy at 100 nM concentrations using near-field scanning optical microscopic (NSOM) geometries and highly diffracting force sensing fiber probes. *Israel J. Chem.* **47**, 171-176.

[83] Lewis, A., Taha, H., Strinkovski, A., Manevitch, A., Khatchatouriants, A., Dekhter, R. and Ammann, E. (2003), Near-field optics: from subwavelength illumination to nanometric shadowing. *Nature Biotech.* **21**, 1378-1386.

[84] Li, X., Zhu, R., Yu, A. and Zhao, X. S. (2011), Ultrafast Photoinduced Electron Transfer between Tetramethylrhodamine and Guanosine in Aqueous Solution. *J. Phys. Chem. B* **115**, 6265-6271.

[85] Liu, Y., Kim, H.-R. and Ahmed A. Heikal. (2006), Structural Basis of Fluorescence Fluctuation Dynamics of Green Fluorescent Proteins in Acidic Environments. *J. Phys. Chem. B*, **110**, 24138-24146.

[86] Losa, G. A. (2009), The fractal geometry of life. *Rivista di Biologia* **102**, 29-59.

[87] Macháň, R. and Hof, M. (2010), Lipid diffusion in planar membranes by fluorescence correlation spectroscopy. Biochim. *Biophys. Acta*, **1798**, 1377-1391.

[88] Macháň, R. and Hof, M. (2011), Recent Developments in Fluorescence Correlation Spectroscopy for Diffusion Measurements in Planar Lipid Membranes. *Int. J. Mol. Sci.* **11**, 427-457.

[89] Magde, D. (1976), Chemical kinetics and fluorescence correlation spectroscopy. *Quart. Rev Biophys.* **9**, 35–47.

[90] Magde, D., Elson E. L. and Webb W. W. (1974), Fluorescence correlation spectroscopy: II. An experimental realization. *Biopolymers* **13**, 29-61.

[91] Magde, D., Elson, E. L. and Webb, W. W. (1972), Thermodynamic fluctuations in a reacting system: measurements by fluorescence correlation spectroscopy. *Phys. Rev. Lett.* **29**, 705–708.

[92] Malchus N., Weiss M. (2010), Elucidating anomalous protein diffusion in living cells with fluorescence correlation spectroscopy-facts and pitfalls. *J. Fluor.* **20**, 19-26.

[93] Malvezzi-Campeggi, F., Jahnz, M., Heinze, K. G., Dittrich, P. and Schwille, P. (2001), Light-induced flickering of DsRed provides evidence for distinct and interconvertible fluorescent states. *Biophys. J.* **81**, 1776-1785.

[94] Manzo, C., van Zanten, T. S. and Garcia-Parajo, M. F. (2011), Nanoscale fluorescence correlation spectroscopy on intact living cell membranes with NSOM probes. *Biophys. J.* **100**, L8-10.

[95] Mashiah A., Wolach O., Sandbank J., Uziel O., Raanani P., Lahav M. (2008), Lymphoma and leukemia cells possess fractal dimensions that correlate with their biological features. *Acta Haematolog*. **119**, 142-150.

[96] Meseth, U., Wohland, T., Rigler, R. and Vogel, H. (1999), Resolution of fluorescence correlation measurements. *Biophys. J.* **76**, 1619–1631.

[97] Miller, A. E., Fischer, A. J., Laurence, T., Hollars, C. W., Saykally, R. J., Lagarias, J. C. and Huser, T. (2006), Single-molecule dynamics of phytochrome-bound fluorophores probed by fluorescence correlation spectroscopy. *Proc. Natl. Acad. Sci. U.S.A.* **103**, 11136-11141.

[98] Mütze, J., Ohrt, T. and Schwille, P. (2011), Fluorescence correlation spectroscopy in vivo. *Laser Photonics Rev.* **5**, 52-67.

[99] Mukhopadhyay, S., Krishnan, R., Lemke, E.A., Lindquist, S. and Deniz, A. A. (2007), A natively unfolded yeast prion monomer adopts an ensemble of

collapsed and rapidly fluctuating structures. *Proc. Natl. Acad. Sci. U.S.A.* **104**, 2649-2654.

[100] N. L. Thompson, in: J. R. Lakowicz (Ed.), Topics in Fluorescence Spectroscopy, vol. 1, Plenum Press, New York, 1991, pp. 337–378.

[101] Nagy A., Wu J., Berland K. M. (2005), Observation volumes and g-factors in two-photon fluorescence fluctuation spectroscopy. *Biophys. J.* **89**, 2077-2090.

[102] Nettels D., Hoffmann A., Schuler B. (2008), Unfolded protein and peptide dynamics investigated with single-molecule FRET and correlation spectroscopy from picoseconds to seconds. *J. Phys. Chem.* B **112**: 6137-6146.

[103] Nettels, D., Gopich, I.V., Hoffman, A. and Schuler, B. (2007), Ultrafast dynamics of protein collapse from single-molecule photon statistics. *Proc. Natl. Acad. Sci. U.S.A.* **104**, 2655-2660.

[104] Neuweiler, H., Doose, S., and Sauer, M. (2005), A microscopic view of miniprotein folding: enhanced folding efficiency through formation of an intermediate. *Proc. Natl. Acad. Sci. U.S.A.* **102**, 16650-16655.

[105] Neuweiler, H., Löllmann, M., Doose, S. and Sauer, M. (2007), Dynamics of unfolded polypeptide chains in crowded environment studied by fluorescence correlation spectroscopy. *J. Mol. Biol.* **365**, 856-869.

[106] Nicolini C., Celli A., Gratton E., Winter R. (2006), Pressure tuning of the morphology of heterogeneous lipid vesicles: a two-photon-excitation fluorescence microscopy study. *Biophys. J.* **91**, 2936-2942.

[107] Oheim, M., Michael, D. J., Geisbauer, M., Madsen, D. and Chow, R. H. (2006), Principles of two-photon excitation fluorescence microscopy and other nonlinear imaging approaches. *Adv. Drug Deliv. Rev.* **58**, 788-808.

[108] Petersen, N. O. (1986), Scanning fluorescence correlation spectroscopy. 1. Theory and simulation of aggregation measurements. *Biophys. J.* **49**, 809-815.

[109] Petrásek, Z. and Schwille, P. (2008b), Photobleaching in two-photon scanning fluorescence correlation spectroscopy. *Chemphyschem* **9**, 147-158.

[110] Petrásek, Z., and Schwille, P. (2008a), Scanning fluorescence correlation spectroscopy. In Single Molecules and Nanotechnology, Vol. 12. Springer Series in Biophysics. R. Rigler and H. Vogel, editors. Springer, Berlin. 83–105.

[111] Pitschke, M., Prior, R., Haupt, M. and Riesner, D. (1998), Detection of single amyloid b-protein aggregates in the cerebrospinal fluid of Alzheimer's patients by fluorescence correlation spectroscopy. *Nature Medicine*, **4**, 832–834.

[112] Purkayastha, P., Klemke, J. W., Lavender, S., Oyola, R., Cooperman, B. S. and Gai, F. (2005), Alpha 1-antitrypsin polymerization: a fluorescence correlation spectroscopic study. *Biochemistry* **44**, 2642-2649.

[113] Rigler Chem Phys. 1999.

[114] Rigler, R. and Widengren, J. (1990a), *Biosci.* **3**, 180-183.

[115] Rigler, R., Mets, U., Widengren, J. and Kask, P. (1990b), Eur. *Biophys. J.* **22**, 169-175.

[116] Ringemann, C., Harke, B., von Middendorff, C., Medda, R., Honigmann, A., Wagner, R., Leutenegger, M., Schonle. A, Hell, S. W., and Eggeling, C. (2009), Exploring single-molecule dynamics with fluorescence nanoscopy. *New J. Phys.* **11**, 103054.

[117] Rogers, J. M. G., Polishchuk, A. L. Guo, L., Wang, J., DeGrado, W. F. and Gai, F. (2011), Photoinduced electron transfer and fluorophore motion as a probe of the conformational dynamics of membrane proteins: application to the influenza A M2 proton channel. *Langmuir*, **27**, 3815–3821.

[118] Rossow, M. J., Sasaki, J. M., Digman, M. A. and Gratton, E. (2010), Raster image correlation spectroscopy in live cells. *Nature Protocols*, **5**, 1761-1774.

[119] Rubart M. (2004), Two-photon microscopy of cells and tissue. *Circulation Research* 95: 1154-1166.

[120] Ruckstuhl, T. and Seeger, S. (2004), Attoliter detection volumes by confocal total-internal-reflection fluorescence microscopy. *Opt. Exp.* **29**, 569-571.

[121] Sahoo, B., Balaji, J., Nag, S., Kaushalya, S. K. and Maiti, S. (2009), Protein aggregation probed by two-photon fluorescence correlation spectroscopy of native tryptophan. *Chem. Phys.* **129**, 075103.

[122] Sanabria, H., Kubota, Y. and Waxham, M. N. (2007), Multiple diffusion mechanisms due to nanostructuring in crowded environments. *Biophys. J.* **92**: 313-322.

[123] Savageau, M. A. (1993), Influence of fractal kinetics on molecular recognition. *J. Mol. Recog.* **6**, 149-157.

[124] Schenk, A., Ivanchenko, S., Röcker, C., Wiedenmann, J. and Nienhaus, G. U. (2004), Photodynamics of red fluorescent proteins studied by fluorescence correlation spectroscopy. *Biophys. J.* **86**, 384-394.

[125] Schwille, P, Haupts U, Maiti S and Webb W. W. (1999), Molecular dynamics in living cells observed by fluorescence correlation spectroscopy with one- and two-photon excitation. *Biophys. J.* **77**, 2251-2265.

[126] Schwille, P. (2001), Fluorescence correlation spectroscopy and its potential for intracellular applications. Cell Biochem. *Biophys.* **34**, 383-408.

[127] Schwille, P. (2002), Fluorescence correlation spectroscopy for the detection and study of single molecules in biology. *Bioessays* **24**, 758-764.

[128] Schwille, P. and Haustein, E. (2004), Fluorescence Correlation Spectroscopy: An introduction to concepts and applications. Biophysical Textbooks online, 1-33.

[129] Schwille, P. and Heinze, K. G. (2001), Two-photon fluorescence cross-correlation spectroscopy. *ChemPhysChem*, **2**, 269-272.

[130] Schwille, P., Meyer-Almes, F. J. and Rigler, R. (1997), Dual-color fluorescence cross-correlation spectroscopy for multicomponent diffusional analysis in solution. *Biophys. J.* **72**, 1878-1886.

[131] Sengupta, P., Garai, K., Balaji, J., Periasamy, N. and Maiti, S. (2003), Measuring size distribution in highly

heterogeneous systems with fluorescence correlation spectroscopy. *Biophys. J.* **84**, 1977-1984.

[132] Seward, H. E. and Bagshaw, C. R. (2009), The photochemistry of fluorescent proteins: implications for their biological applications. *Chem. Soc. Rev.* **38**, 2842-2851.

[133] Sherman, E., Itkin, A., Kuttner, Y. Y., Rhoades, E., Amir, D., Haas, E. and Haran, G. (2008), Using fluorescence correlation spectroscopy to study conformational changes in denatured proteins. *Biophys. J.*, **94**, 4819-4827.

[134] Slaughter B. D., Allen, M. W., Unruh, J, R., Urbauer, R. J. B. and Johnson, C. K. (2004), Single-molecule resonance energy transfer and fluorescence correlation spectroscopy of calmodulin in solution. *J. Phys. Chem. B*, (need page number).

[135] Szymanski J., Weiss M. (2009), Elucidating the origin of anomalous diffusion in crowded fluids. *Phys. Rev. Lett.* **103**, 038102.

[136] Tcherniak, A., Reznik, C., Link, S. and Landes, C. F. (2009), Fluorescence Correlation Spectroscopy: Criteria for Analysis in Complex Systems. *Anal. Chem.* **81**, 746–754.

[137] Thompson, N. L. and Steele, B. L. (2007), Total internal reflection with fluorescence correlation spectroscopy. *Nature Protocols*, **2**, 878-890.

[138] Thompson, N. L., Wang, X., Navaratnarajah, P. Total internal reflection with fluorescence correlation spectroscopy: Applications to substrate-supported planar membranes. *J. Struct. Biol.* **168**, 95-106.

[139] Tjernberg, L. O., Pramanik, A., Björling, S., Thyberg, P., Thyberg, J., Nordstedt, C., Berndt, K. D., Terenius L. and Rigler, R. (1999), Amyloid beta-peptide polymerization studied using fluorescence correlation spectroscopy. *Chem. Biol.* **6**, 53-62.

[140] Torres T., Levitus M. (2007), Measuring conformational dynamics: a new FCS-FRET approach. *J. of Phys. Chem. B* **111**, 7392-7400.

[142] Tsay, J. M. Doose, S, and Weiss, S. (2006), Rotational and Translational Diffusion of Peptide-Coated CdSe/CdS/ZnS Nanorods Studied by Fluorescence Correlation Spectroscopy. *J. Amer. Chem. Soc.* **128**, 1639-1647.

[143] Vobornik, D., Banks, D. S., Lu, Z., Fradin, C., Taylor, R. and Johnston, L. J. (2008), Fluorescence correlation spectroscopy with sub-diffraction-limited resolution using near-field optical probes. *Appl. Phys. Lett.* **93**, 163904, (1-2).

[144] Wachsmuth, M., Waldeck, W. and Langowski, J. (2000), *J. Mol. Biol.* **298**, 677-689.

[145] Wawrezinieck, L., Rigneault, H., Marguet, D. and Lenne, P. F. (2005), Fluorescence correlation spectroscopy diffusion laws to probe the submicron cell membrane organization. *Biophys. J.* **89**, 4029–4042.

[146] Webb, W. W. (1976), Applications of fluorescence correlation spectroscopy. *Quart. Rev. Biophys.* **9**, 49–68.

[147] Weidemann, T., Wachsmuth, M., Tewes, M., Rippe, K. and Langowski, J. (2002), Analysis of ligand binding by two-colour fluorescence cross-correlation spectroscopy. *Single Mol.* **1**, 49-61.

[148] Weiss, M., Elsner, M., Kartberg, F. and Nilsson, T. (2004), Anomalous subdiffusion is a measure for cytoplasmic crowding in living cells. *Biophys. J.* **87**, 3518-3524.

[149] Wenger, J. and Rigneault, H. (2010), Photonic methods to enhance fluorescence correlation spectroscopy and single molecule fluorescence detection. *Int. J. Mol. Sci.* **11**, 206-221.

[150] Widengren, J., Mets, U. and Rigler R. (1995). Fluorescence correlation spectroscopy of triplet states in solution: A theoretical and experimental study. *J. Phys. Chem.* **99**, 13368-13379.

[151] Widengren, J., Mets, U. and Rigler R. (1999), Photodynamic properties of green fluorescent proteins investigated by fluorescence correlation spectroscopy. *Chem. Phys.* **250**, 171-186.

[152] Wilkins, D. K., S. B. Grimshaw, V. Receveur, C. M. and Dobson, J. A. (1999), Hydrodynamic radii of native and denatured proteins measured by pulse field gradient NMR techniques. *Biochemistry*, **38**, 16424–16431.

[153] Winckler, P., Jaffiol, R., Plain, J. and Royer, P. (2010), Nonradiative Excitation Fluorescence: Probing Volumes Down to the Attoliter Range J. Phys. *Chem. Lett.* **1**, 2451–2454.

[154] Wu, J. and Berland, K. M. (2008), Propagators and time-dependent diffusion coefficients for anomalous diffusion. *Biophys. J.* **95**, 2049-2052.